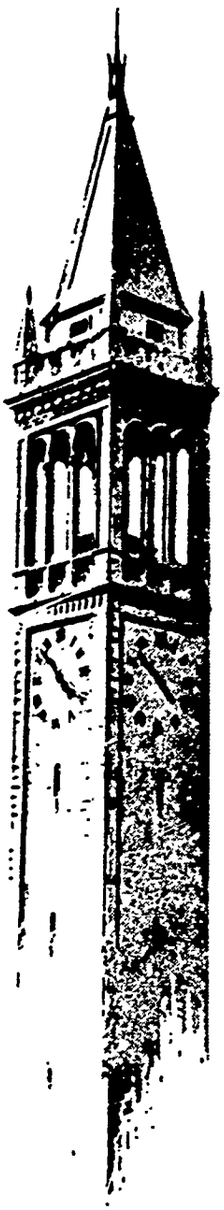

FLAME PROPAGATION RATES IN THE COMBUSTION OF AMMONIA

by

G. S. Samuelsen

Report No. TS-65-4
Contract DA-04-200-AMC-791(X)
September 1965

INSTITUTE OF ENGINEERING RESEARCH

UNIVERSITY OF CALIFORNIA
Berkeley, California

University of California
Department of Mechanical Engineering
Heat Power Systems

FLAME PROPAGATION RATES IN THE COMBUSTION OF AMMONIA

by

G. S. Samuelsen

TECHNICAL REPORT NO. 5

Under Contract
DA-04-200-AMC-791 (x) Ammonia Fuel

ARMY MATERIEL COMMAND
R&D DIRECTORATE

Chemistry and Materials Branch

Project Director
E. S. Starkman

September 9, 1965

TABLE OF CONTENTS

LIST OF TABLES

LIST OF FIGURES

NOMENCLATURE

BMEP	-	Brake Mean Effective Pressure
BTDC	-	Before Top Dead Center
^{o}F	-	Degrees Fahrenheit
fps	-	feet per second
IMEP	-	Indicated Mean Effective Pressure
ms	-	milliseconds
psig	-	pounds per square inch gauge
rpm	-	revolutions per minute
TDC	-	Top Dead Center
o	-	crank angle degrees
ϕ	-	equivalence ratio

ABSTRACT

Flame Propagation Rates in the Combustion of Ammonia

Gary Scott Samuelsen

Degree of Master of Science Mechanical Engineering

An investigation has been made of the flame propagation rates and peak pressures of ammonia as compared to iso-octane in spark ignition engine combustion.

The influence of compression ratio, speed, manifold pressure, and dissociation of ammonia prior to combustion was studied as a function of equivalence ratio (ϕ). The ammonia kernel development proved to be 1.4 times greater than the 2.72 millisecond average recorded with iso-octane. The maximum ammonia flame rate was 59 fps at $\phi = 0.85$ and, for iso-octane, 83 fps at $\phi = 1.23$. While the propagation rates of iso-octane fell uniformly on either side of maximum, the ammonia flame rates dropped rapidly on the rich side of maximum through an inflection point. Prior partial dissociation of ammonia, before introduction to the engine was found to be of prime importance to flame speeds, becoming more critical for leaner mixtures.

INTRODUCTION

During the past year, an investigation has been under way in the Department of Mechanical Engineering at the University of California, to investigate ammonia as a fuel for combustion engines. This research has been under contract to the Army Materiel Command and resulted from an ability to obtain ammonia directly from a nuclear-powered depot process (Ref. 12). It was the desire of the government to use the ammonia as a fuel for operating vehicles and for space heating.

Success was achieved in operating a Waukesha Cooperative Fuel Research (CFR) spark-ignition engine with ammonia in the vapor phase injected directly into the manifold. Seventy-three percent of the 158 IMEP resulting from the use of iso-octane was realized. This is eight percent short of the theoretical as predicted during the initial stages of the project. Obtainment of this power level necessitated dissociating the ammonia by means of a high temperature (900°F) catalyst. It was concluded therefore that hydrogen was necessary for successful engine operation. It was hypothesized that this prior dissociation provided the means for initiating dissociation among the remaining species during compression and in the normal combustion process. Only in this manner was it possible to operate the engine smoothly and at optimum power. This is due, in part, to the high inflammability range of hydrogen (4.0 to 75.0 percent by volume - Ref 4) to which the combustion of ammonia must be largely contributed. Experience and equipment limitations dictated an initial dissociation range of three to five percent hydrogen by weight.

Ammonia as a fuel exhibits unique characteristics. Optimum combustion required a spark advance nearly two-fold greater than the 30-40 degree advance used with iso-octane or other hydrocarbons. The question was raised whether longer kernel development (Figure 1), prolonged flame propagation (Figure 2), or a combination of both caused the required variation in spark timing. In addition, ammonia displayed no dependence on spark advance over a large range of values throughout the lean region. These phenomena initiated interest in a flame propagation rate study.

An analytical procedure to predict flame propagation rates, even for such simple systems as hydrogen and oxygen, in either closed or open systems, has been completely unsuccessful to date (Ref. 4). For this reason, this study is highly empirical, but does embody a broad spectrum of experimental parameters. Hopefully, the results will be useful in allowing others to confirm future analytical approaches relating to ignition and flame speeds in ammonia-air systems at high temperatures and pressures.

LONGER KERNEL DEVELOPMENT ILLUSTRATION

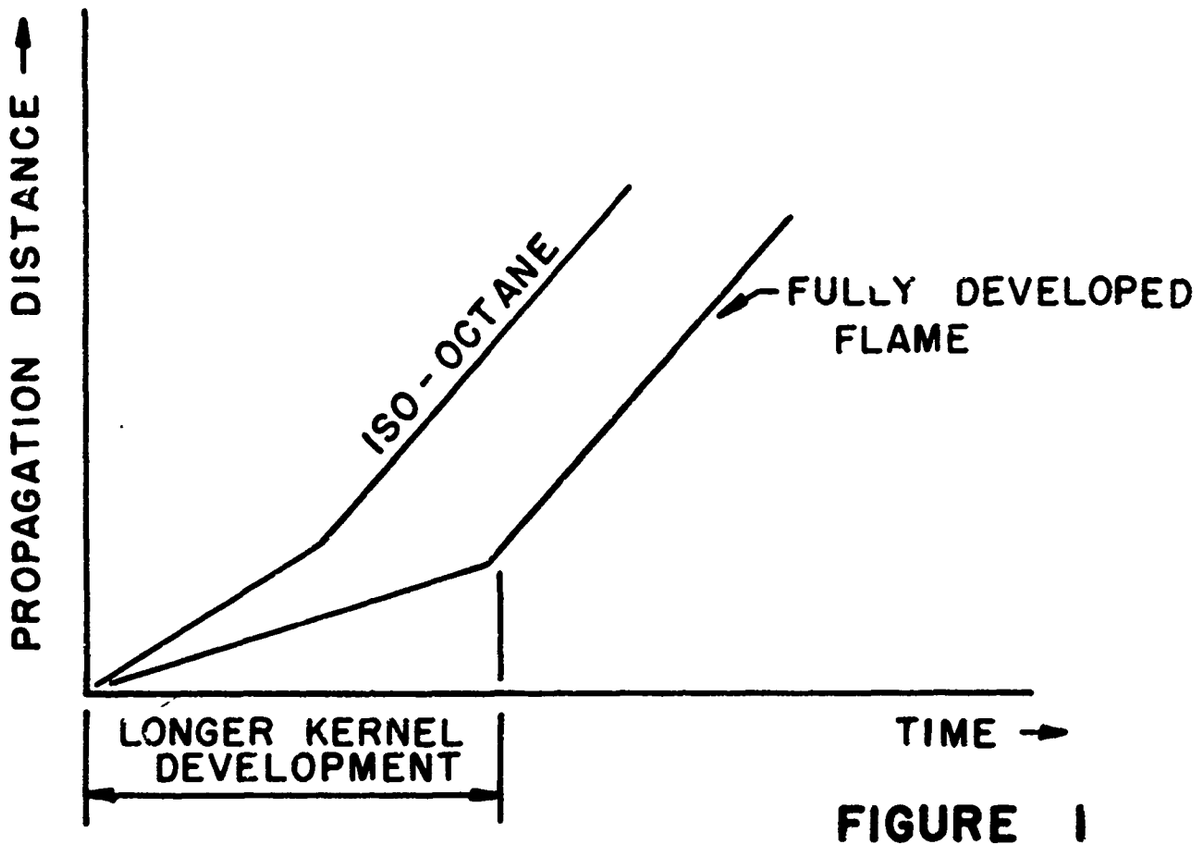

FIGURE 1

SLOW FLAME SPEED ILLUSTRATION

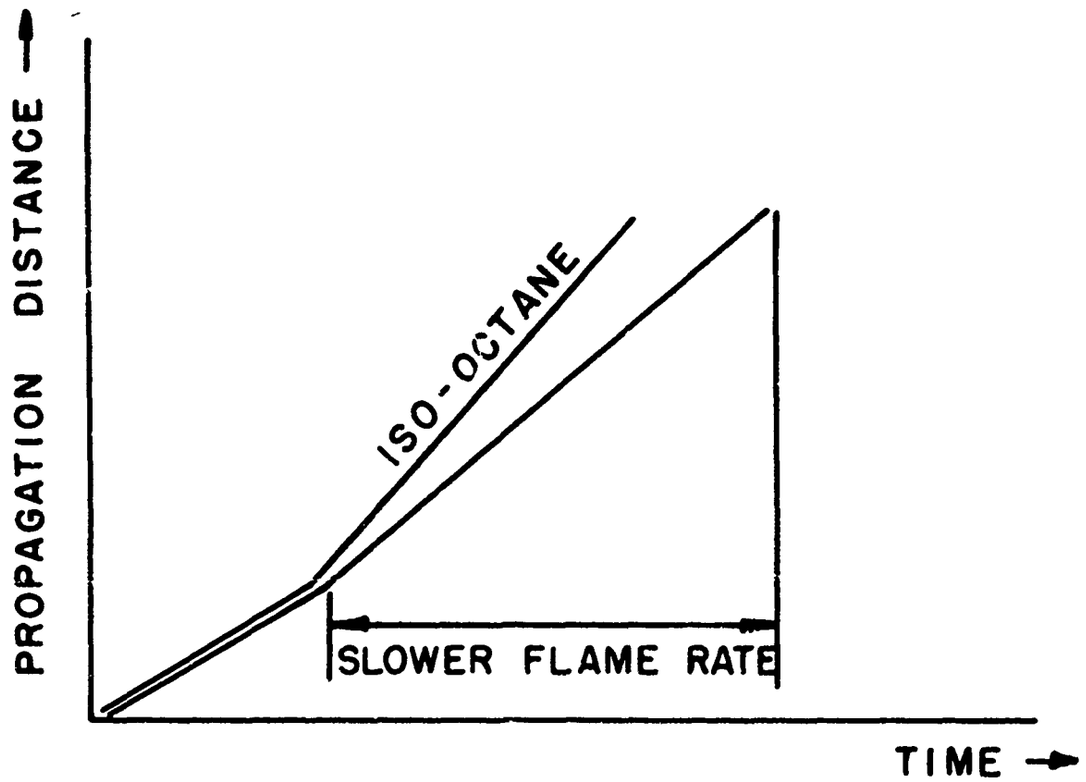

FIGURE 2

BASIC CONSIDERATIONS

Ionization gaps were selected as the devices for studying the flame propagation rates. With a specified voltage imposed upon the gap, current will flow when a given concentration of ionized molecules of the gas is in the space between the electrodes. The resulting breakdown can be monitored, and the occurrence of ionization determined.

The ionized gases which cause the current to flow are generally conceded to be certain species produced as intermediates in the combustion process. Because of the present difficulty in identifying these species in combustion gases, it is only possible to speculate upon the character of the ions present in the flame front. Through experimental work with hydrocarbons, however, H_3O^+ has been identified as the most abundant ion (Ref. 7). If nitrogen is involved in the reaction, NO^+ ions also tend to become substantial, as other ions transfer their charge to the nitric oxide molecules (Ref. 13).

No work has ever been undertaken to analyze extensively the intermediate species in ammonia combustion. It was found by De Jaegere (Ref. 13) that a flame propagating in a NH_3:O_2 mixture produced a very small amount of ions which conforms to the experimental evidence produced in this study. The ions were identified as NO^+ and NH_4^+.

EXPERIMENTAL RESEARCH

I. The Engine

A standard CRF supercharge engine (Ref 1) was chosen for the experimental work (Fig. 3). The layout of the ionization gaps and the type of head were specially selected for this investigation. Prior work had been done at the University using an L-head cylinder (Refs. 3 & 11), but this did not allow the variation in compression ratio the study required. Strong consideration was given to modifying a CFR split-head cylinder in a manner adopted by S. Curry in a 1962 study (Ref 2). Experimental work soon showed that sensitivity of the gaps to shorting made this configuration impractical.

The final decision was made to use a modified CFR four-hole cylinder head which allowed the placement of five ionization gaps, a spark plug, and a pressure transducer. Champion N-8 14 mm extended-reach spark plugs were used for the ionization gaps. due to their compatibility with the construction of the head. The ground electrodes were removed to avoid potential pre-ignition hot spots and to provide a symmetrical target for the approaching flame front. Figure 4 shows four ion gaps in place. For the iso-octane runs a Champion UD-16 spark plug was used and for ammonia, a RJ-11. Figure 5 shows the configuration of the gaps in the cylinder head. The bore of the cylinder was $3\frac{1}{4}$ inches and the stroke of the standard crankshaft was $4\frac{1}{2}$ inches. The resulting engine displacement was 37.4 in^3. The power output generated by the engine was absorbed in a resistor bank connected to a Sprague cradle dynamometer with which it was possible to hold the speed of the engine to $\pm$ 2% by a manual control.

The standard CFR air metering system was used (Ref 1). The fuel metering facilities for the iso-octane and ammonia are described in Appendixes A and B respectively. A U-tube measuring device provided a determination of flow rate when using iso-octane. The ammonia flow was monitored continuously, being indicated by a Cox turbine flow-meter. As a check, the ammonia was also measured volumetrically by means of a sight glass mounted on the pressurized ammonia supply tank (Fig. 29). Inlet air was furnished by the laboratory compressed air system, heated to 125°F for metering, and delivered to the engine at 100°F and a manifold pressure controllable through a regulator valve. The engine was maintained at 154°F for the iso-octane runs (by the evaporation and condensation of methanol), and at 360°F for ammonia (using an ethylene-glycol-water mixture).[1]

II. Data-Recording System

A principal concern was for efficient and effective data recording. Since it was intended to average many engine cycles for each run, tape recording systems were studied. However, it became more realistic to display the ionization signals on five channels of a two-gun, six channel oscilloscope with the pressure output being imposed on the remaining channel. A Tektronix Type 565 with suitable plug-in units was chosen. A simultaneous display of the pressure-time and flame-time histories of any one particular cycle was recorded photographically by a Dumont oscilloscope Land camera using Poloroid Type 46L film. The recording equipment is shown in Figure 6.

---

1. It was hypothesized that the iron cylinder head acted as a catalyst itself in dissociating the ammonia, and its effect was enhanced with the increased temperature.

Amplification and shaping of the ionization signals was considered. A circuit developed by T. Dahm (Ref 3) was used as a basis for the analysis. Because a multi-channel oscilloscope was being used, shaping the signals for the purpose of identification as done previously, was not necessary. Shaping would merely clarify the display and cut out the ragged ionization signal. Were a special circuit to be used, the dependence of the triggering mechanism on the ionization signal would cause unavoidable and inconsistant errors. A significant cycle-to-cycle variation in signal (Fig. 7) exists as well as a great difference in output between the two fuels being studied (Fig. 8).[2] Thus, the special shaping electronics were not used. Instead, the voltage drop in the ion gap was monitored directly.

Because of the high voltage potential induced on the ionization plug (1000 to 1500 volts d.c.) it was not appropriate to locate the oscilloscope input directly across the gap. The final circuit design (Figs. 9 and 10 - a spare sixth channel is shown) allowed the input signal to be drawn off a leg parallel to the ionization gap and across a resistance at a low potential. The recording of the actual ionization signal greatly enhanced the ability of the investigator to interpret the data.

A Kistler Corporation crystal pressure transducer (Type 601A) and Type S/N 1455 Charge Amplifier were used to observe the pressure history of the combustion cycle. The pickup was housed in a water-cooled adapter and exposed to combustion gases through one of the seven holes in the modified head (Fig. 6).

---

2. As an interesting sidelight, it was determined that iso-octane created a 3.3 greater voltage drop than ammonia under similar operating conditions. The ionization potential of iso-octane proved to be much higher than that of ammonia.

III. Experimental Procedure

The CFR engine is well instrumented for efficient and accurate data determination. The flexibility of the system provides close control over the variables appropriate to the fuel research work: Spark advance, compression ratio, speed, manifold inlet temperature and pressure, and fuel and air flow rates.

The initial hour of operation was devoted to engine warm-up and to insuring that the equipment was functioning properly. Upon the attainment of steady state, the following engine operating data were recorded: fuel flow rate, air flow rate, air inlet temperature and manifold pressure, engine cooling jacket temperature, spark advance, speed, compression ratio, BMEP, FMEP, and, in the case of ammonia, the amount of dissociation.[3] The variables included in this study were the air and fuel flow rates, compression ratio, speed, manifold pressure, and ammonia dissociation. The following conditions were maintained for all runs:

Air pressure at metering orifice:	40 psig
Air temperature at metering orifice:	125°F
Engine cooling jacket temperature:	
Iso-octane:	154°F
Ammonia:	360°F
Engine oil temperature:	165°F

The run schedule is outlined in Table I. For each set of conditions, ten single-sweep pictures were taken of the five ionization signals and one pressure display. A typical photograph is shown in Fig. 11, with one ionization signal impc d on each of five channels. The initial noise within the first graduation is a result of the ignition which initiates

3. A Beckman Gas Chromotograph was used to determine hydrogen dissociation by weight. A one cubic centimeter sample was taken from the ammonia intake line for all runs as the standard volume.

the sweep. A few of the ionization signals can be shown reflecting signal responses from another channel. This is easily interpreted from observing the actual voltage drop due to ionization.

IV. Data Reduction

Because of the obvious cycle-to-cycle variation in pressure and flame travel, averaging was chosen. Of course, more than ten representative pictures would have been desired for this process, but the number was restricted by the time available for reading. The pictures were read on a Lehner-Benson Oscar N-2 at the Lawrence Radiation Laboratory in Berkeley. This data analyzer reads and prints coordinate points from magnified oscilloscope photographs onto IBM cards.[4] A computer program was formulated to average the flame front and pressure points and produce results appropriate to the propagation study. The value of the Oscar as a tool to determine accurately the time-history of the output characteristics cannot be over-estimated. The card output of the analyzer greatly facilitated the computer data reduction process. More than 80 engine conditions were recorded and 1100 pictures averaged.

The physical distance between ionization gaps were measured beforehand; thus the flame-front propagation rate was determined by a direct plot of the data. Figure 12 illustrates such a plot of both average flame speed and pressure data for one fuel-to-air ratio.

---

4. The Oscar has two long "cross-hair" arms, one vertical and one horizontal. The arms are moved manually to cross at a position for which the coordinate points are desired. Pressing a button punches these points on cards relative to a 0-10,000 preset scale.

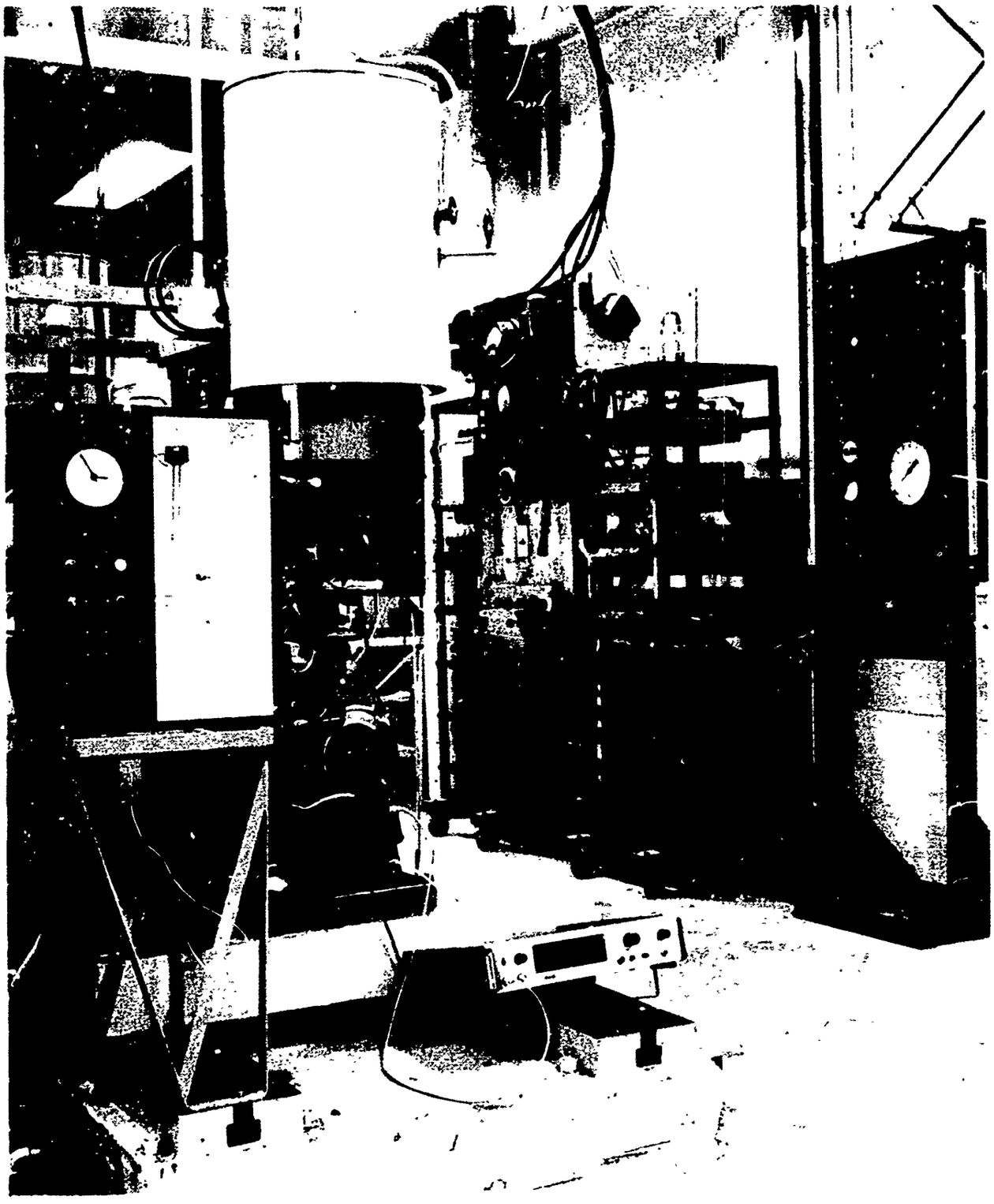

View of CFR Engine Facility FIGURE 3

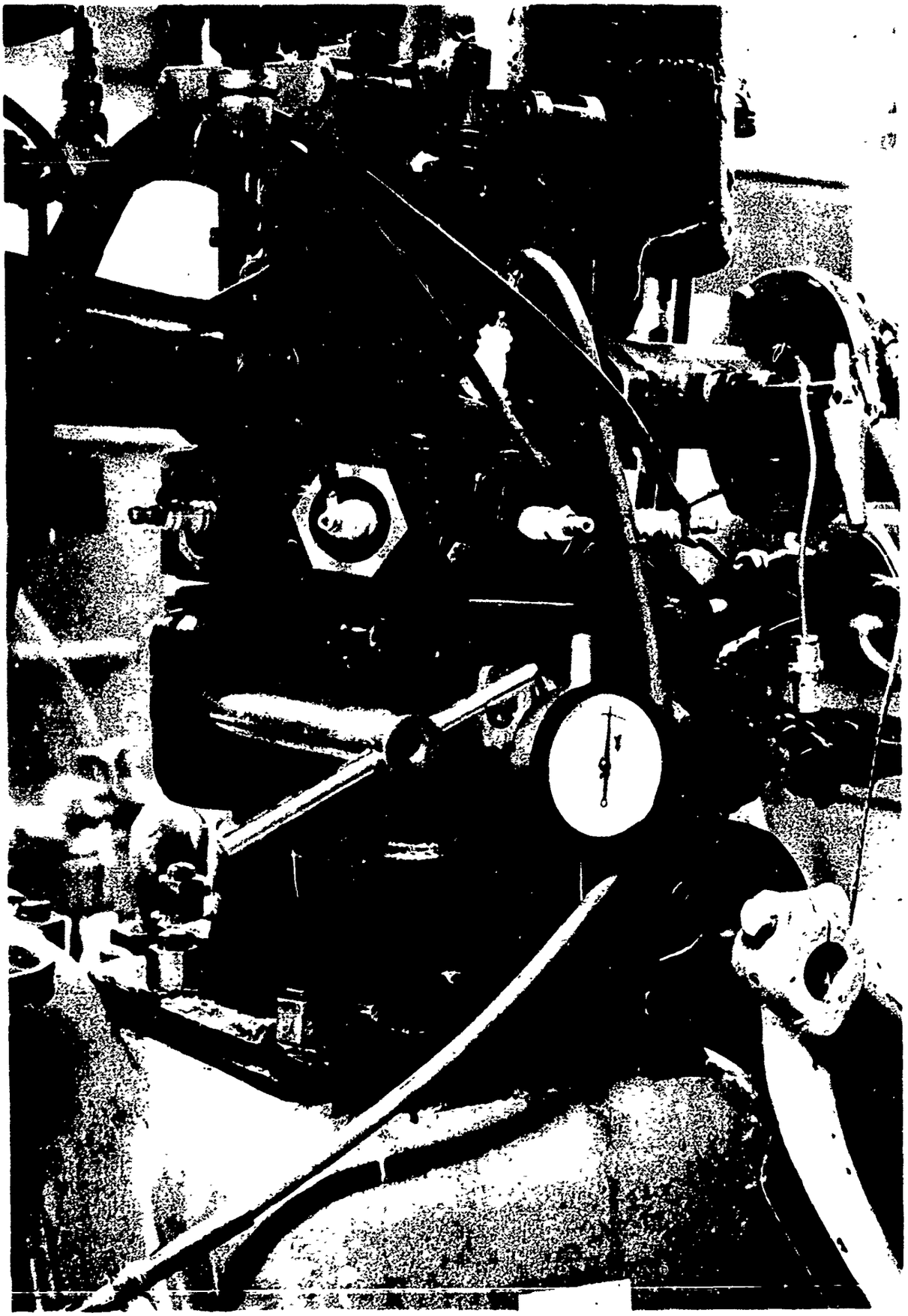

View of Four Ion Gaps in Place FIGURE 4

DISTANCE FROM SPARK - FT.

a	0.058
b	0.107
c	0.110
d	0.187
e	0.187
f	0.251

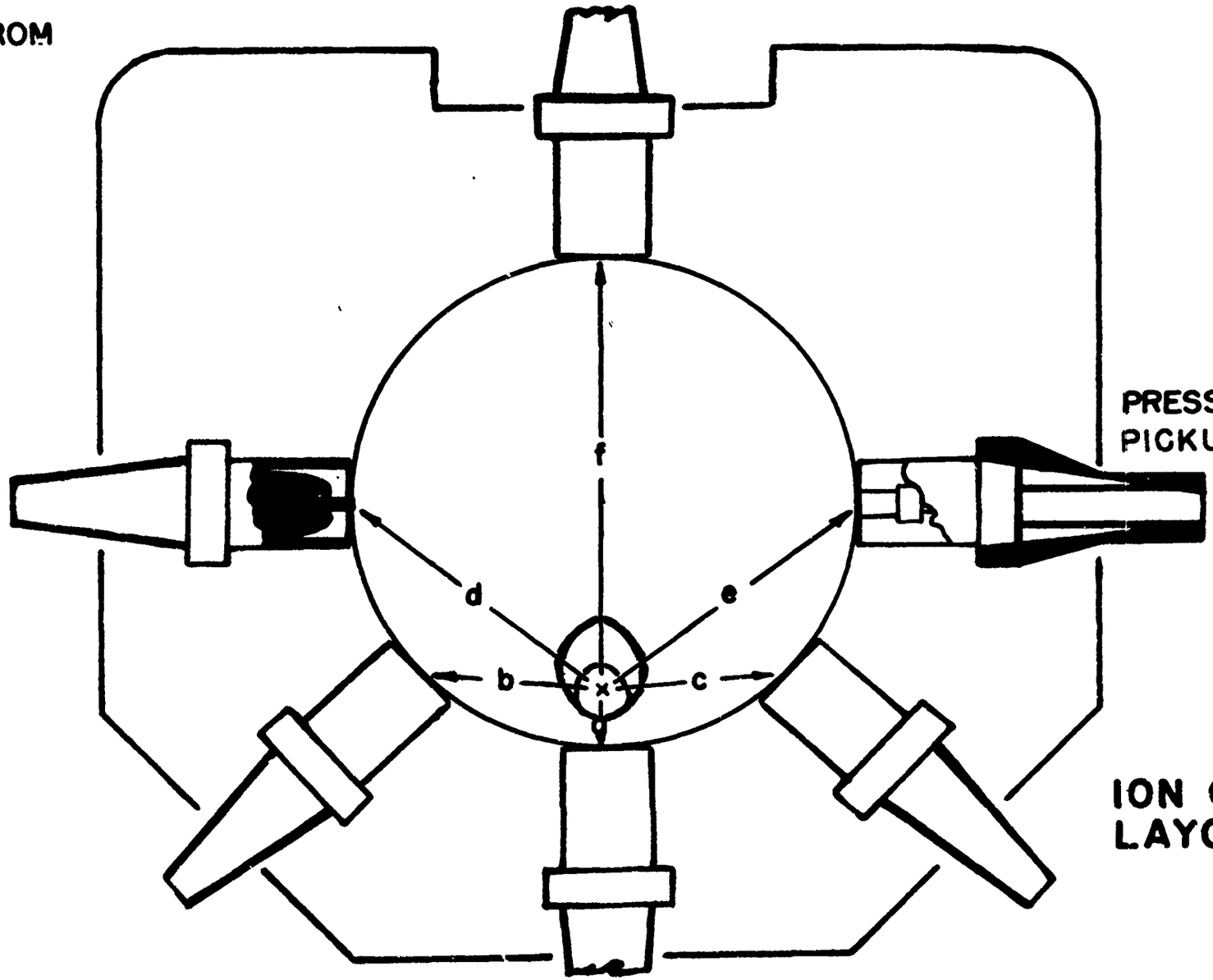

FIGURE 5

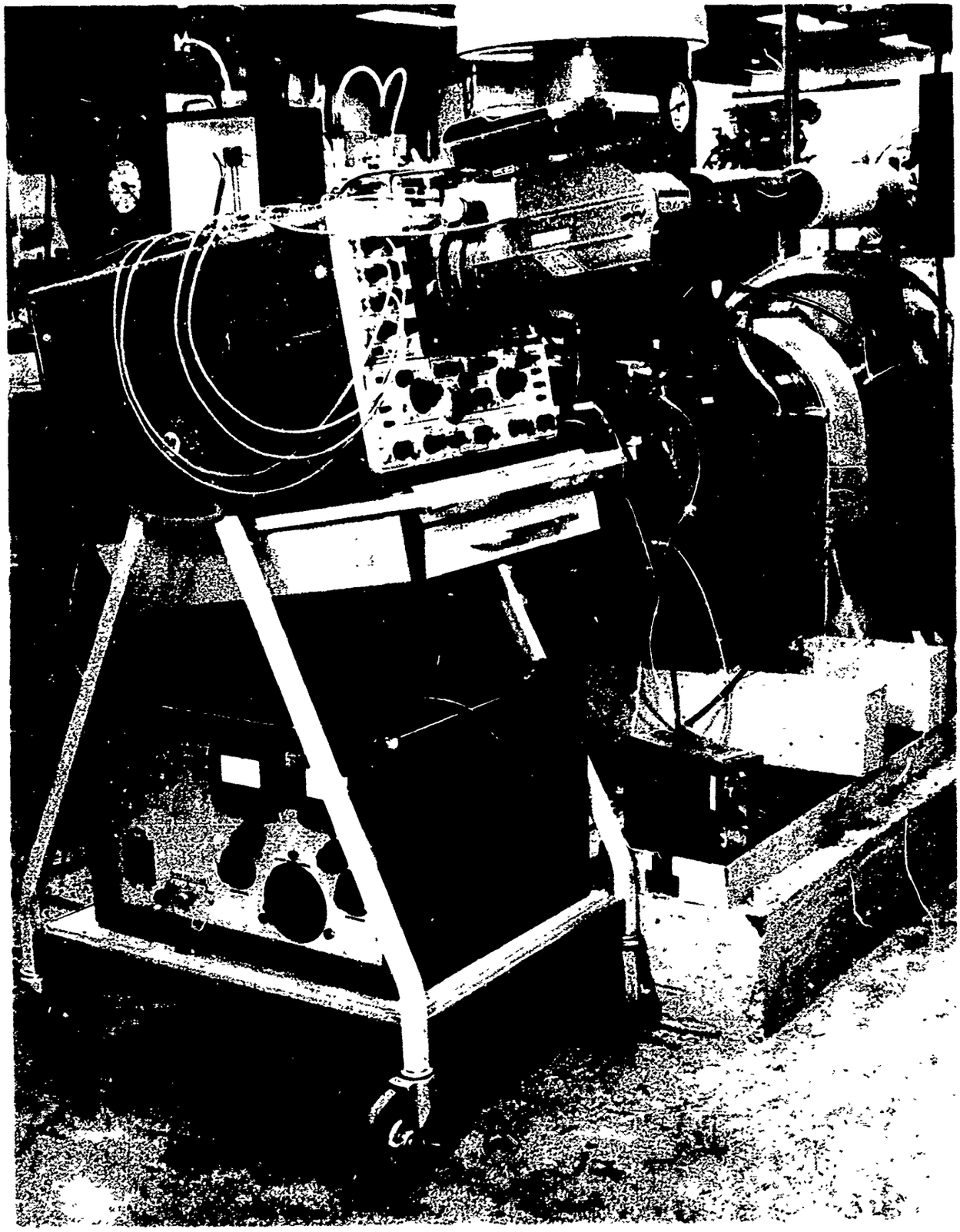

View of Recording Equipment FIGURE 6

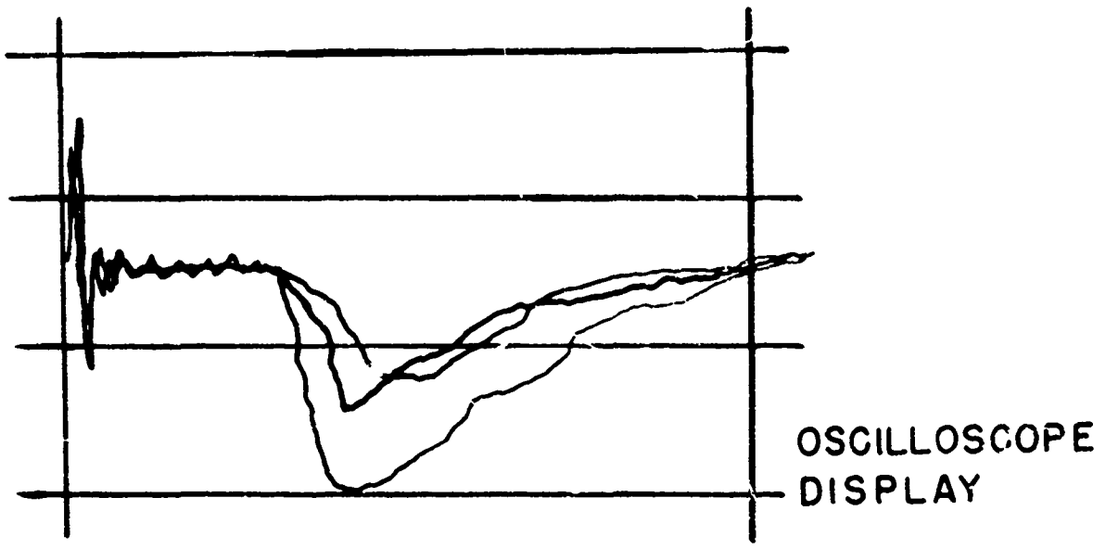

CYCLE TO CYCLE VARIATION IN IONIZATION

FIGURE 7

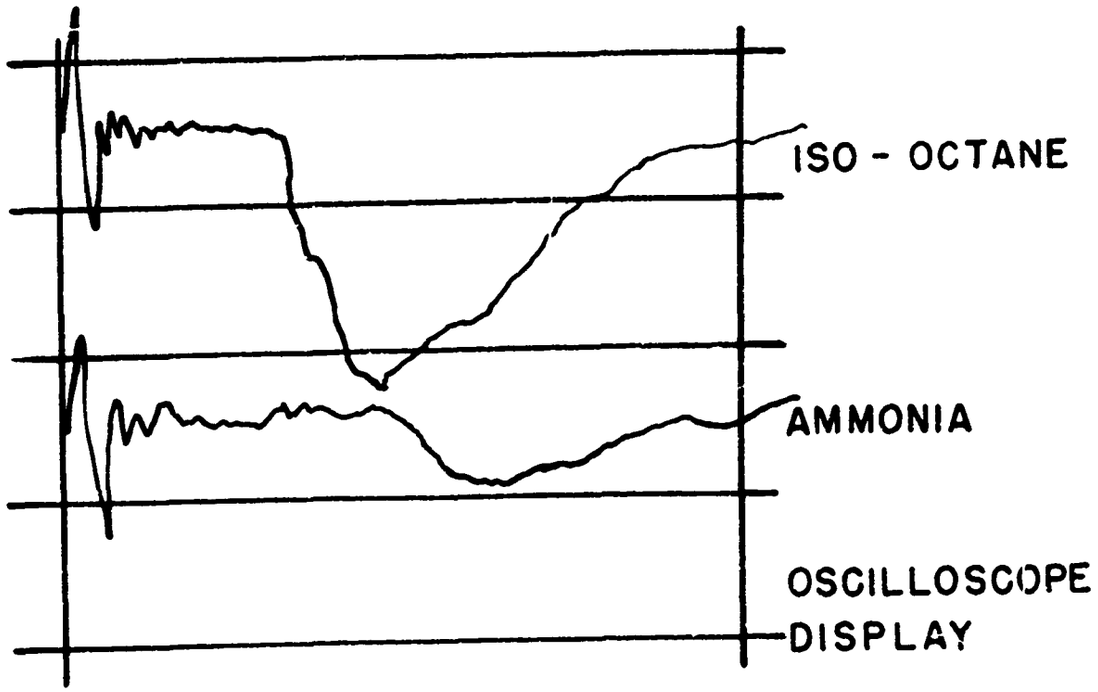

FUEL TO FUEL VARIATION IN IONIZATION

FIGURE 8

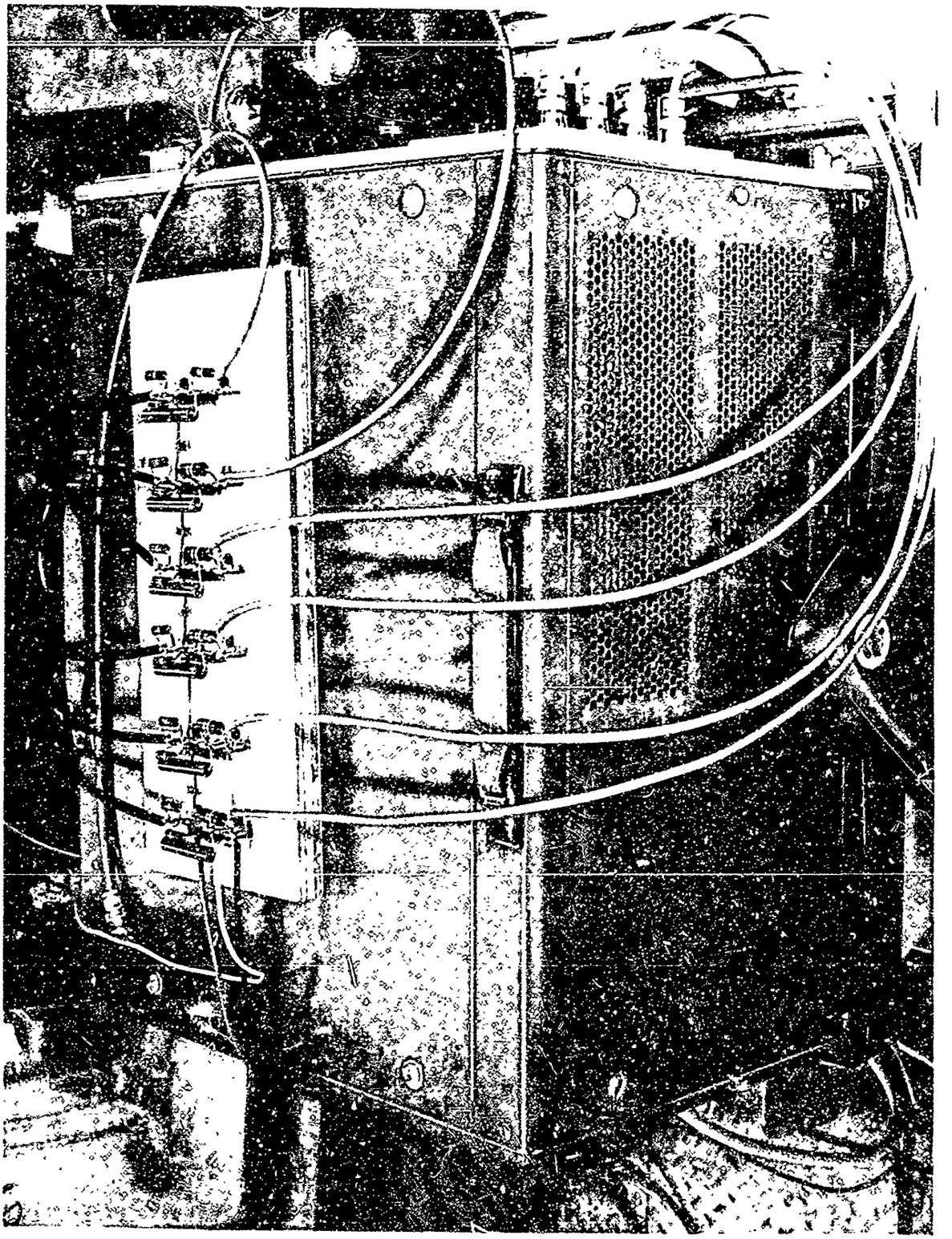

View of Ionization Circuit

FIGURE 10

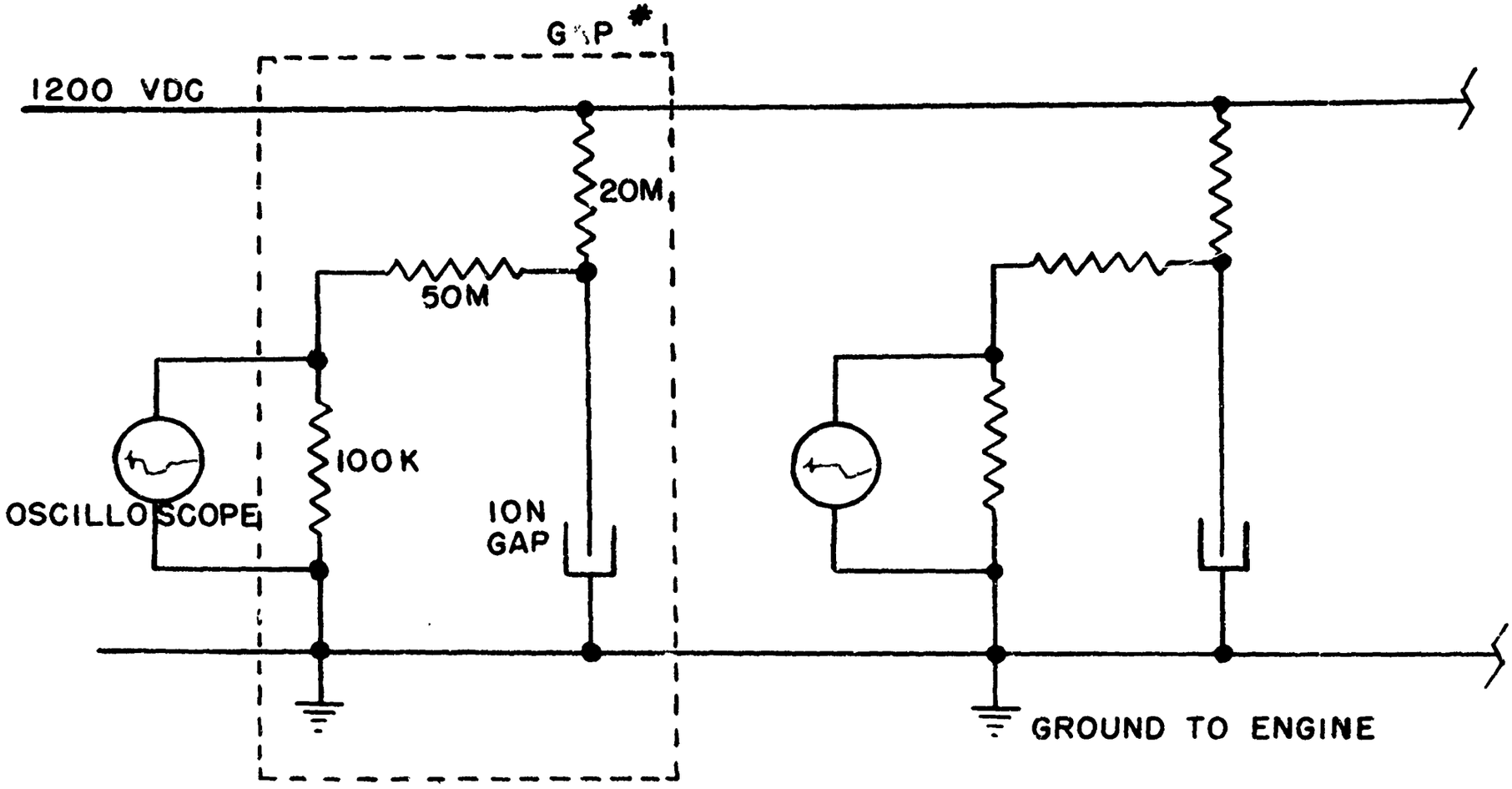

CIRCUIT DIAGRAM

FIGURE 9

TABLE I

RUN	FUEL	COMPRESSION RATIO	EQUIVALENCE RATIO	MANIFOLD PRESSURE in merc	SPEED rpm	SPARK ADVANCE	AMMONIA DISSOCIATION
1	iso-octane	10:1	vary	30	1800	optimum	
2	iso-octane	6:1	vary	30	1800	optimum	
3	iso-octane	8:1	vary	30	1800	optimum	
4	iso-octane	8:1	vary	30	1300	optimum	
5	iso-octane	8:1	vary	30	1000	optimum	
6	iso-octane	8:1	vary	21	1800	optimum	
7	iso-octane	8:1	vary	30	1800	vary	
8	iso-octane	8:1	vary	21	1800	vary	
11	ammonia	10:1	vary	30	1800	optimum	maximum
12	ammonia	8:1	vary	30	1800	optimum	maximum
13	ammonia	6:1	vary	30	1800	optimum	maximum
15	ammonia	8:1	vary	30	1800	vary	maximum
16	ammonia	8:1	vary	30	1300	optimum	maximum
17	ammonia	8:1	vary	30	1800	optimum	vary
19	ammonia	8:1	vary	30	1000	optimum	maximum
20	ammonia	8:1	vary	21	1800	optimum	maximum
21	ammonia	8:1	vary	21	1800	vary	maximum

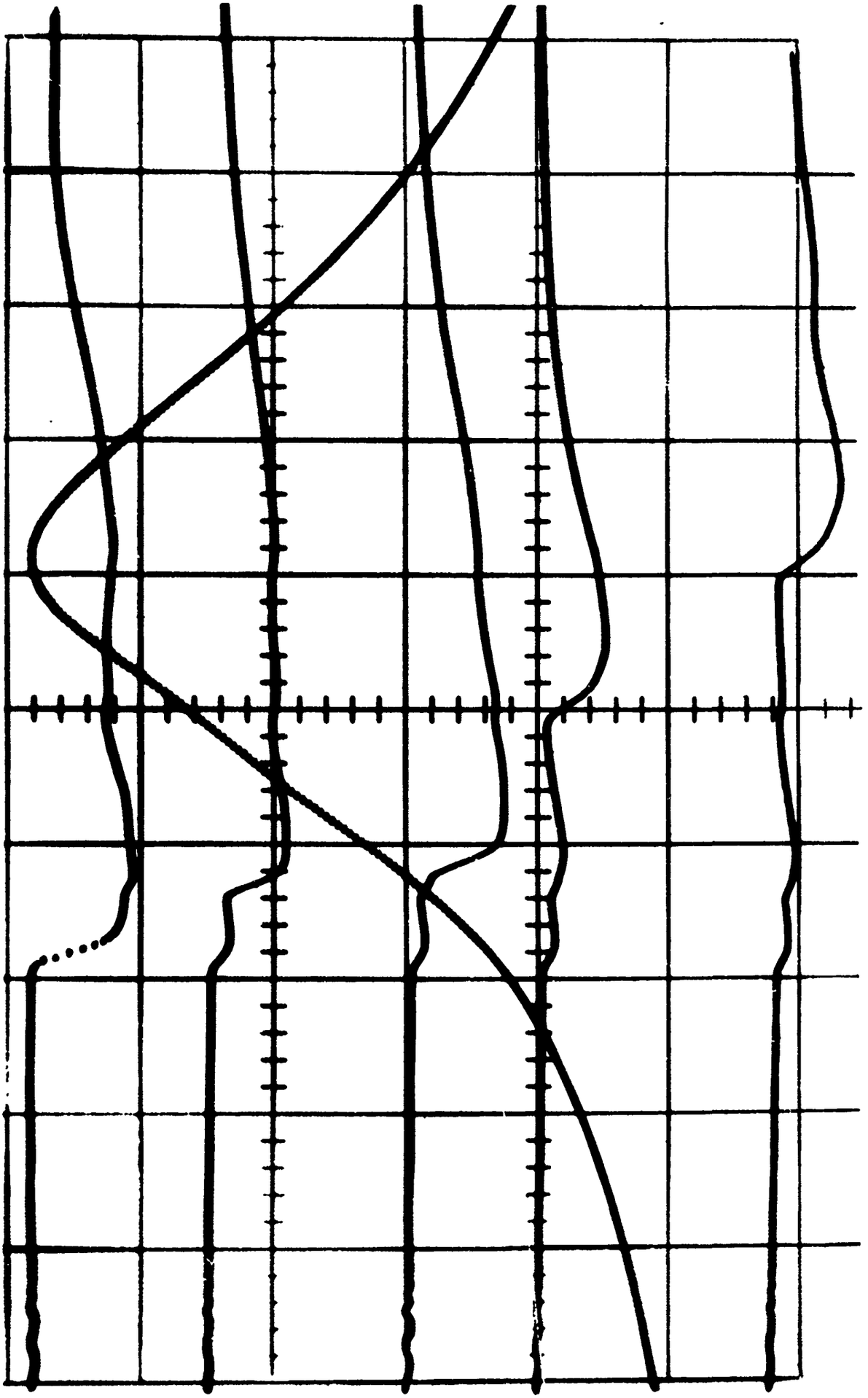

Typical Photographic Record of Ionization and Pressure

FIGURE 11

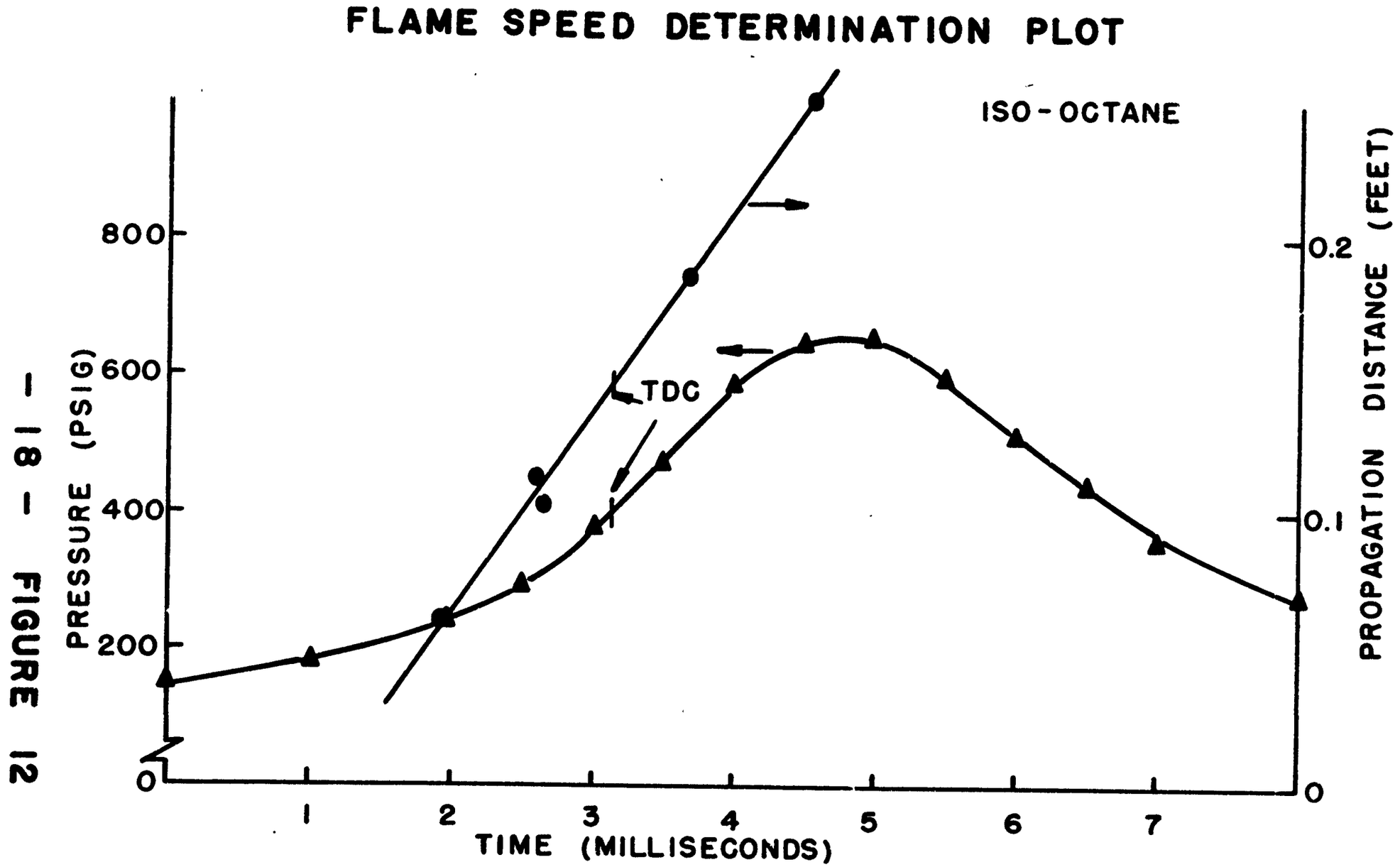
FLAME SPEED DETERMINATION PLOT
ISO-OCTANE
TDC
PRESSURE (PSIG)
800
600
400
200
0
PROPAGATION DISTANCE (FEET)
0.2
0.1
0
1
2
3
4
5
6
7
TIME (MILLISECONDS)

FIGURE 12 - 18 -

EXPERIMENTAL RESULTS AND DISCUSSION

It was the objective of this study to better understand the unusual characteristics in spark time resulting from the combustion of ammonia by comparing the flame propagation rates to those of iso-octane. In addition, pressure-time histories were to be recorded as an aid in explaining the ammonia combustion phenomena. The results are tabulated in Table II for iso-octane and Table III for ammonia.

Flame Propagation Rates:

Ammonia flame rates yield striking differences to those found with iso-octane. The fully developed flame front propagates more slowly than that of iso-octane (59 fps compared to 83 fps at the maximum). Moreover, the kernel development period of ammonia is substantially longer than that of iso-octane. These two characteristics, true of the majority of runs completed in this investigation[5], are illustrated in Fig. 14 for ammonia and iso-octane under similar running conditions. The first ion gap (0.058 feet from the spark plug) frequently showed evidence of being within the kernel development period. Thus, the extrapolation of the flame propagation line through the 0.050 foot coordinate (Fig. 14) was chosen as the datum for the kernel development comparisons. In Fig. 13, the kernel development distribution is plotted as a function of occurrence frequency (per 0.5 ms intervals) over all the 80 runs undertaken in this study. It is readily observable that the average development time for ammonia (3.79 ms) is significantly longer than the average for iso-octane (2.72 ms). Consequently, the increased spark advance necessitated in the burning of

---

5. In the extreme lean region, the ammonia flame rates approached and sometimes rose above those of the iso-octane (Fig. 15). The kernel development, however, remainded substantially longer.

ammonia is a reflection of both a slower propagation rate and delayed kernel development time.

Fig. 15 shows the flame speed plotted as a function of fuel/air ratio for three compression ratios: 10:1, 8:1, and 6:1.[6] The iso-octane contours have a continuous curvature whereas the ammonia exhibits an inflection point similar to the nitroparaffin fuels (Ref. 11). The hydrocarbon fuel is limited by misfire on both sides of the curve. The performance curves for ammonia are determined by loss of power at the extremes, not misfire. The ionization and pressure outputs reflect a greater cycle-to-cycle continuity than iso-octane.

The flame propagation rates show a definite dependence upon the compression ratio. This is to be expected from basic thermodynamic principles. Therefore, both fuels should maintain the same contour throughout the range of compression ratios. It is evident that ammonia operates satisfactory over less than one half of the iso-octane range from ϕ = 0.6 to 1.1. Iso-octane peaks at an equivalence ratio between 1.1 and 1.3. Maximum propagation rates occur in ammonia in the leaner region of 0.8 to 0.9. The equivalence ratio at which top flame speed occurs increases for both fuels as the compression ratio increases although ammonia maintains a narrower range of equivalence ratios.

Engine speed affects both the contour and magnitude of the flame-speed spectrum for ammonia and iso-octane (Fig. 18). The curves tend

---

6. There was insufficient ionization at the extreme lean mixtures. In order to complete the ammonia flame and pressure curves and indicate the extent to which it was possible to operate the engine on lean, a "starred" point has been chosen arbitrarily. Please note that propagation rate and pressure information was not recorded at these points. The magnitude of the equivalence ratio is the only basis of validity.

to expand their effective range and flatten as the speed is decreased from 1800 rpm to 1000. Ammonia in particular, displays a more regular contour at 1000 rpm while decreasing less with speed than iso-octane. There was a 1.5 fold decrease for ammonia as compared to a 1.85-fold decrease for iso-octane. Preconditioning of the mixture during compression is probably the most significant variable in this phenomena.[7]

Decreasing the manifold pressure from 30 inches of mercury to 21 inches clearly lowers the iso-octane flame rates from 74.1 fps to 67.9 (Fig. 21). The ammonia contour loses curvature rather than exhibiting a flame speed decrease below 52.5 fps. Curiously, one might expect the ammonia flame rates to decrease with this change in manifold pressure. The pressure effect on the propagation rates has been shown in Fig. 15 where a definite decrease is evident. There does exist one possible explanation. At the lower manifold pressure, the ammonia dissociation was over 5% for all points. This value varied between 3.70 and 5% at 30 inches of mercury because of the limitations of the ammonia dissociation equipment.[8]

The effect of ammonia dissociation on the flame speed proved to be of prime importance. Figure 24 shows the flame speeds as a function of equivalence ratio for various dissociation levels. Figure 25 is a cross plot of Fig. 24. There exists a significant increase in the flame speed

---

7. Performance curves, comparing IMEP to equivalence ratio and illustrating dependence on the key variables used in this study are included in Figs 17, 20, and 23.

8. The lower manifold pressure demands a decreased fuel flow rate. This increases the effective time of catalyst exposure and results in a consequent dissociation increase. This is also true for all runs as the charge progresses to leaner values.

between three and four percent dissociation of hydrogen by weight. In Fig. 24, a gradual decrease in the positive slope between two and three percent is observed to progress into an opposite trend at four percent. The dependence of this observation upon fuel/air ratio is portrayed in Fig. 25. The dependence is greatest at the lean mixtures where the flame rate increases from 40.3 to 49.8 fps but is non-existent at the richer readings. The lean mixtures apparently are more dependent on hydrogen. A specified amount of dissociation is necessary for efficient utilization of the mixture to be realized (for these conditions, 4.0%). Above this initiating value, increased dissociation results in little improvement in flame speed. The richer mixtures, on the other hand, seem less reflective of the influences of prior dissociation and of little influence in varying the flame speed. This characteristic places much more importance on prior dissociation than was previously considered.

The trends level out at their maximum value (53.0 fps for ϕ = 0.79) which indicates that there exists a dissociation percentage above which an increase in flame speed cannot be expected. In this case, 5 percent represents the near-optimum. This value is then probably sufficient to initiate maximum dissociation of the remaining fuel through the normal combustion process.

It was very early noted that spark advance would not greatly vary power output. The probable reason is shown in Fig. 25. It can be seen that the controlling function was the amount of ammonia which had been dissociated to hydrogen.

The dependence of the flame speed upon the dissociation would generally tend to invalidate the data for all runs due to the inability

during the project experimentation to control the dissociation. This was found to affect the lower manifold pressure runs. However, for the most part, there are some saving factors:

1. The only region for which the dissociation magnitude fell significantly below a critical value was the rich.[8] From Fig. 24, it can be seen that the dependence is a minimum. Moreover,

2. the continuity is sufficiently good from run to run, and condition to condition, that trends can be concluded.

Pressure Histories:

The peak pressures give the same inflection characteristics as the flame propagation rates when viewed as a function of equivalence ratio. (Fig. 16). However, the change with compression ratio is not so similar, especially between 6:1 and 8:1 where iso-octane drops 25% from 655 psig to 490. The contours also exhibit less curvature than those found with the flame speed. The ammonia peak pressure trend does not follow that of the performance (IMEP) curves (Fig. 17). This presents an anomaly. However, it must be remembered that the IMEP is a measurement of the area within the pressure-volume plot. Because the volume-time relationships are identical throughout one run, the pressure-time curve may be used as a rough indication of IMEP. When this is taken into account, the IMEP plot does, in fact, portray the continuity that was recorded. In Fig. 26, five pressure curves are shown for differing equivalence ratios.. The area under each is shown graphically in Fig. 27. A comparison of this to Fig. 17 shows correspondence between the two methods of measurement. The lean mixtures produce a fast rising

pressure in the vicinity of the pressure peak, while the rich charges yield an early, slowly rising response.[9] Note especially curve 'd' which corresponds to the inflection region in the peak pressure plot.

The optimum equivalence ratio (Fig. 19) for maximum peak pressure progresses to a leaner value with decreasing engine speed, for both fuels. It must be noted that the maximum for ammonia does not rise below 1300 rpm, but continues at 540 psig to 1000 rpm. These trends do not reflect dependence on the flame rates as a function of speed, but may be the result of the additional energy release due to the extended time for combustion.

A decrease in manifold pressure (Fig. 22) shows a definite drop in peak pressure which is to be expected. When the spark was optimized at the lean and rich limits, the maximum pressures were increased for both fuels. The effect was greater for iso-octane than for ammonia. The influence on flame velocity was more pronounced at a 21-inch manifold pressure for iso-octane than at 30 inches. The opposite was true for ammonia.

---

9. Although the area determination should be considered over the full cycle, because the initial pressure was identical in each case, and nearly identical at 18 ms, this range was chosen.

TABLE II

ISO-OCTANE

RUN	COMPRESSION RATIO	SPEED rpm	MANIFOLD PRESSURE in merc	FLAME SPEED fps	PEAK PRESSURE psig	EQUIVALENCE RATIO
1a	10:1	1800	30	82.0	735	1.23
1b	10:1	1800	30	79.8	710	1.48
1c	10:1	1800	30	42.3	480	1.92
1d	10:1	1800	30	60.8	680	.86
1f	10:1	1800	30	28.4	395	.67
2a	6:1	1800	30	67.2	490	1.08
2b	6:1	1800	30	60.2	470	1.51
2c	6:1	1800	30	49.6	335	1.68
2d	6:1	1800	30	56.0	435	.93
2e	6:1	1800	30	27.2	185	.75
3a	8:1	1800	30	73.9	655	1.14
3b	8:1	1800	30	74.1	650	1.21
3c	8:1	1800	30	59.2	542	1.65
3d	8:1	1800	30	64.9	605	1.58
3e	8:1	1800	30	61.8	620	.94
3f	8:1	1800	30	21.1	290	.68
3h	8:1	1800	30	72.7	650	1.34
3j	8:1	1800	30	46.2	389	1.81
4a	8:1	1300	30	55.0	680	1.09
4b	8:1	1300	30	41.9	420	1.61
4c	8:1	1300	30	50.3	585	1.39
4d	8:1	1300	30	51.9	575	.95
4e	8:1	1300	30	18.5	175	.68
4f	8:1	1300	30	25.0	130	2.01
4g	8:1	1300	30	31.4	300	.76
5b	8:1	1000	30	39.5	725	1.00
5d	8:1	1000	30	19.3	310	.70
5e	8:1	1000	30	23.8	460	.75
5f	8:1	1000	30	21.6	300	1.88
5g	8:1	1000	30	34.4	525	1.54
6a	8:1	1800	21	67.9	560	1.13
6b	8:1	1800	21	53.4	345	.87
6e	8:1	1800	21	62.0	401	1.48
6f	8:1	1800	21	54.5	295	1.68
7d	8:1	1800	30	49.8	399	.71
7e	8:1	1800	30	50.1	580	1.82
8b	8:1	1800	21	64.1	475	.85
8d	8:1	1800	21	62.5	390	1.70

TABLE III

AMMONIA

RUN	COMPRESSION RATIO	SPEED rpm	MANIFOLD PRESSURE in merc	FLAME SPEED fps	PEAK PRESSURE psig	HYDROGEN DISSOCIATION by weight %	EQUIVALENCE RATIO
11a	10:1	1800	30	54.5	560	3.3	.95
11b	10:1	1800	30	50.0	500	3.1	1.01
11c	10:1	1800	30	48.5	470	2.3	1.11
11d	10:1	1800	30	58.4	620	3.6	.88
11f	10:1	1800	30	57.4	630	5.0+	.75
12a	6:1	1800	30	43.6	290	4.2	.86
12b	6:1	1800	30	37.2	265	3.7	.95
12c	6:1	1800	30	33.4	221	3.1	1.06
12e	6:1	1800	30	44.9	285	4.0	.80
13a	8:1	1800	30	48.5	460	3.7	.93
13b	8:1	1800	30	43.2	385	3.3	1.08
13c	8:1	1800	30	46.0	395	3.7	1.01
13d	8:1	1800	30	52.5	485	3.5	.83
13f	8:1	1800	30	48.4	480	4.8	.72
15b	8:1	1800	30	48.7	395	3.5	1.08
16a	8:1	1300	30	40.4	540	4.8	.96
16b	8:1	1300	30	35.2	505	4.4	1.04
16d	8:1	1300	30	45.0	530	5.0+	.74
16e	8:1	1300	30	43.9	565	4.8	.90
16h	8:1	1300	30	32.9	465	5.0+	1.18
17a	8:1	1800	30	39.2		2.0	.94
17b	8:1	1800	30	42.8		3.0	.94
17c	8:1	1800	30	49.0		4.0	.94
17e	8:1	1800	30	45.3		3.5	1.04
17f	8:1	1800	30	44.3		3.0	1.04
17g	8:1	1800	30	43.2		2.0	1.04
17h	8:1	1800	30	34.9		2.0	.79
17i	8:1	1800	30	40.3		3.0	.79
17j	8:1	1800	30	49.8		4.0	.79
17k	8:1	1800	30	52.7		5.0	.79
19a	8:1	1000	30	32.2	515	5.0+	.98
19b	8:1	1000	30	21.3	350	5.0+	1.44
19c	8:1	1000	30	25.1	430	5.0+	1.22
19g	8:1	1000	30	29.5	480	5.0+	.67
19i	8:1	1000	30	33.5	530	5.0+	.89
20a	8:1	1800	21	48.5	310	5.0+	.99
20b	8:1	1800	21	.5	215	4.8	1.06
20d	8:1	1800	21	44.9	275	5.0+	1.01
20e	8:1	1800	21	54.5	280	5.0+	.70
20g	8:1	1800	21	51.4	300	5.0+	.87
20h	8:1	1800	21	46.2	295	5.0+	.93
21a	8:1	1800	21	47.0	225	4.8	1.06

FREQUENCY DISTRIBUTION OF KERNEL DEVELOPMENT

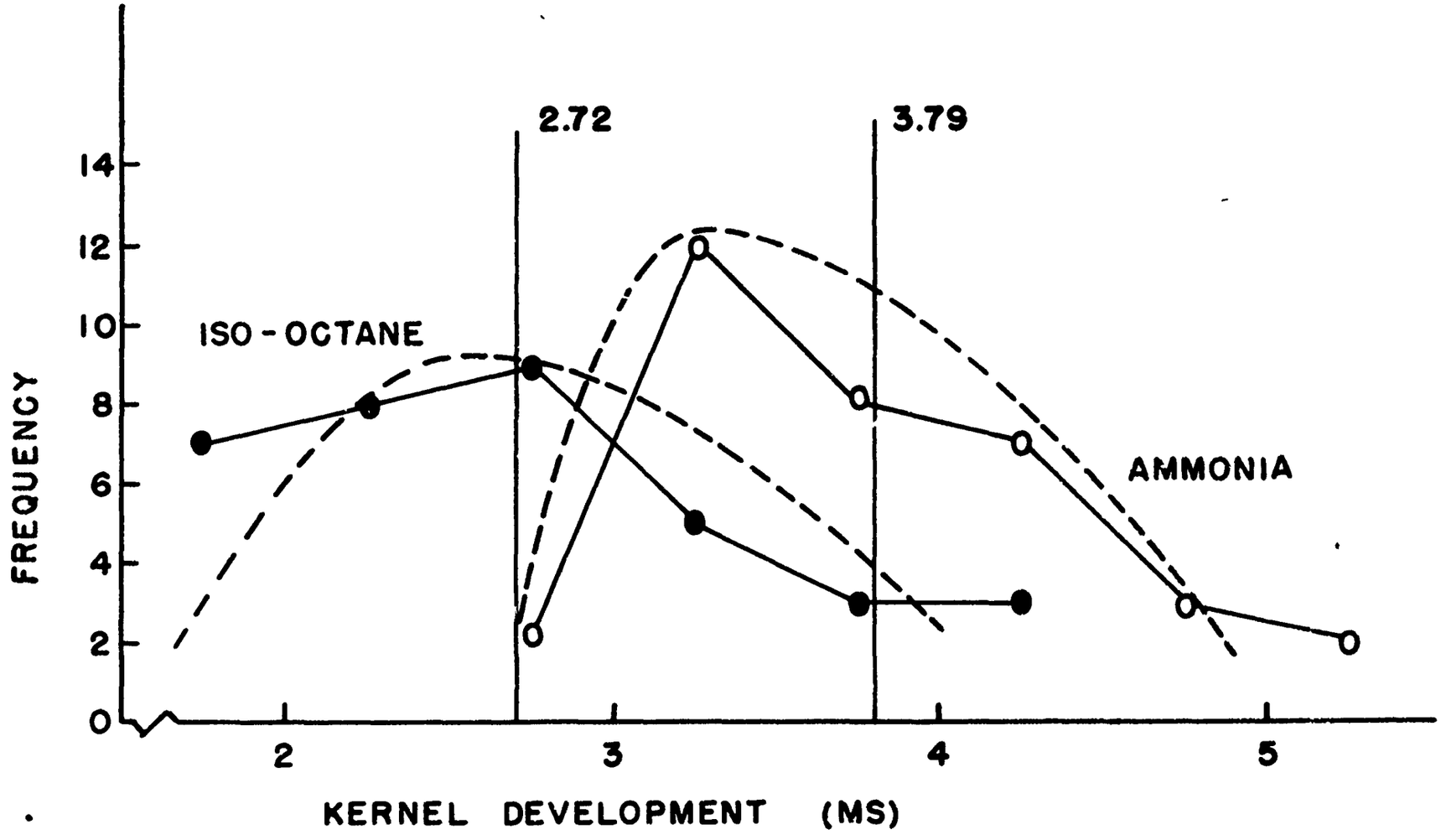

FIGURE 13

THE INFLUENCE OF COMPRESSION RATIO ON FLAME RATE

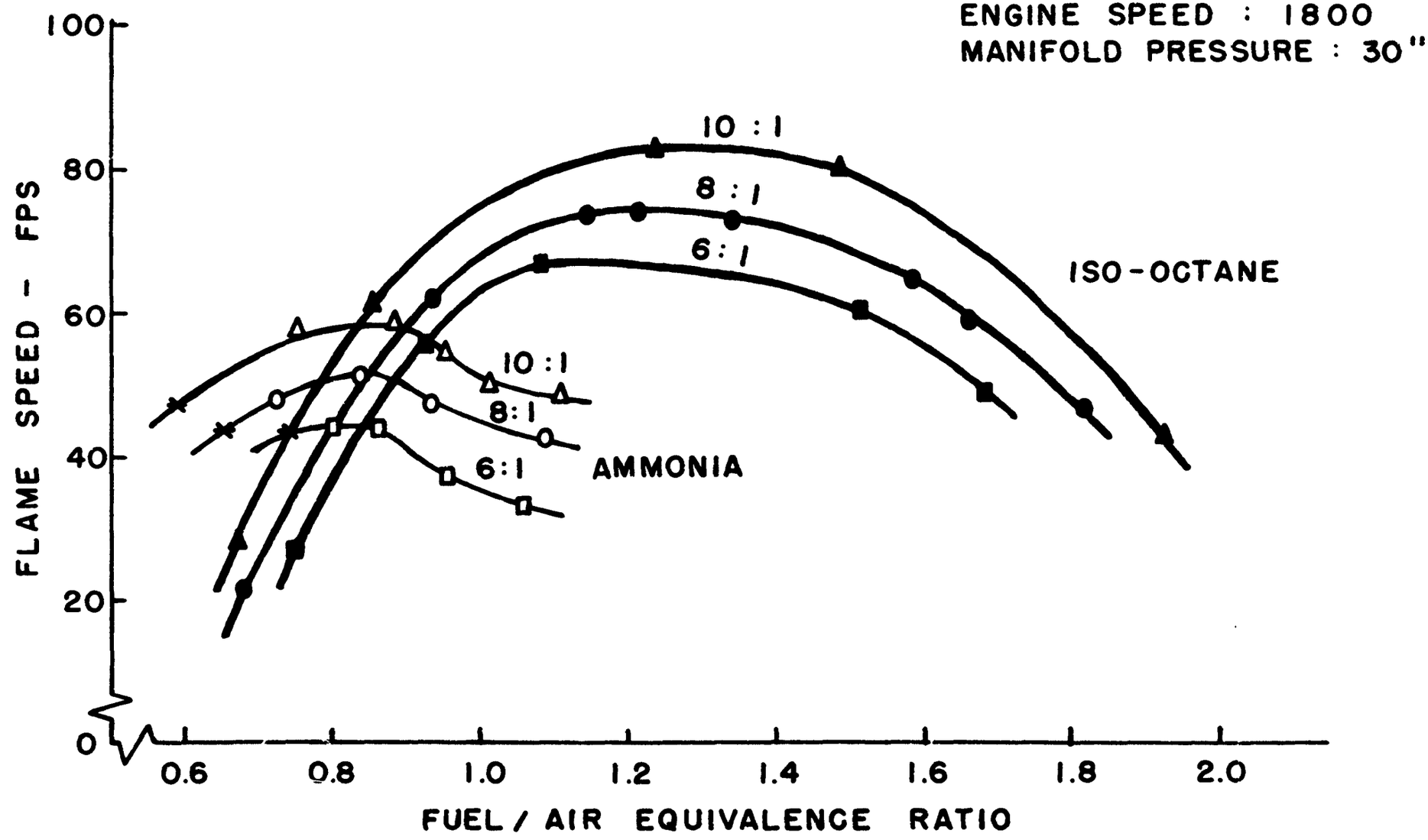

FIGURE 15

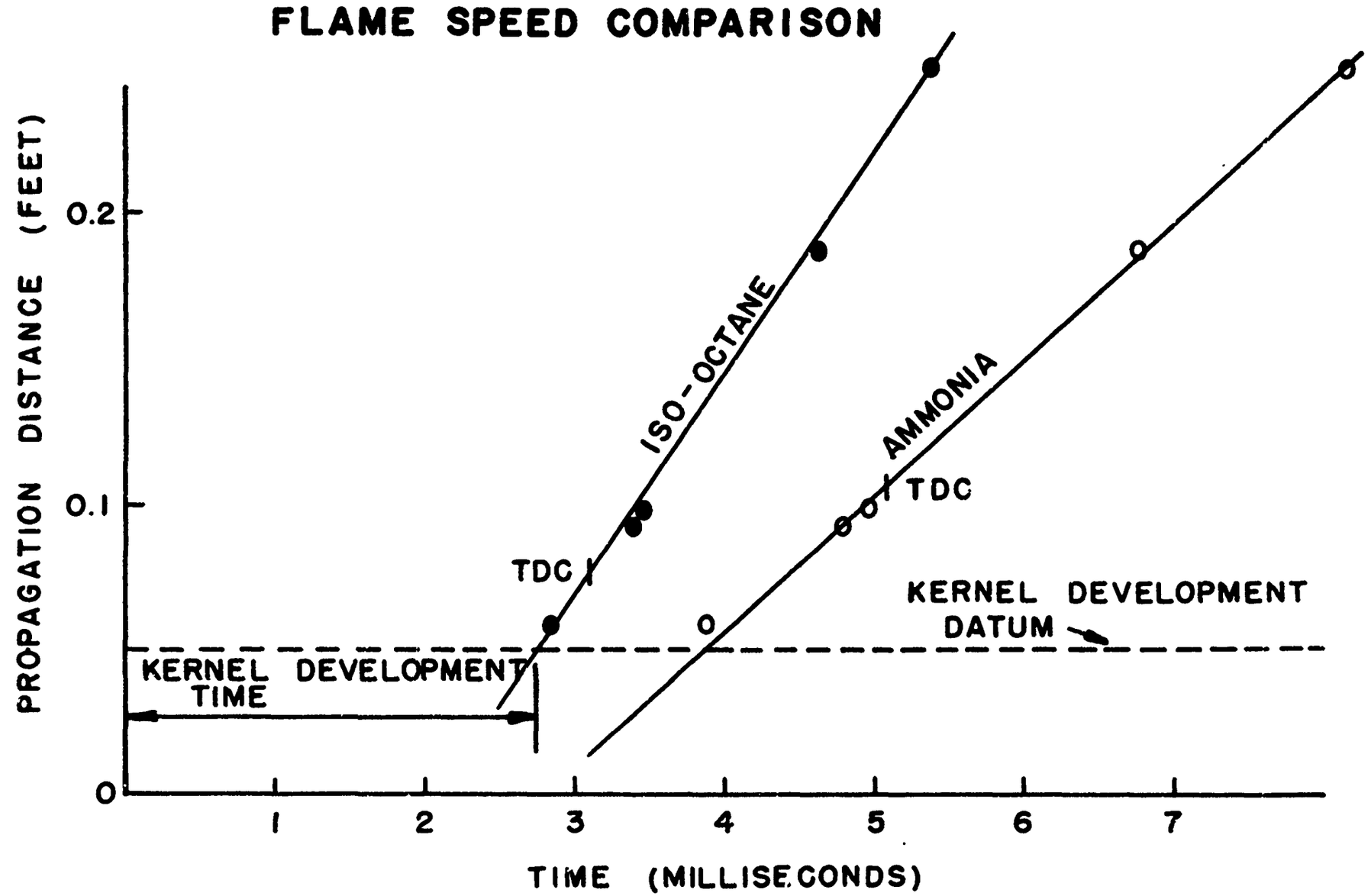
FLAME SPEED COMPARISON
PROPAGATION DISTANCE (FEET)
0.2
0.1
0
ISO-OCTANE
AMMONIA
TDC
TDC
KERNEL DEVELOPMENT DATUM
KERNEL DEVELOPMENT TIME
1
2
3
4
5
6
7
TIME (MILLISECONDS)

FIGURE 14

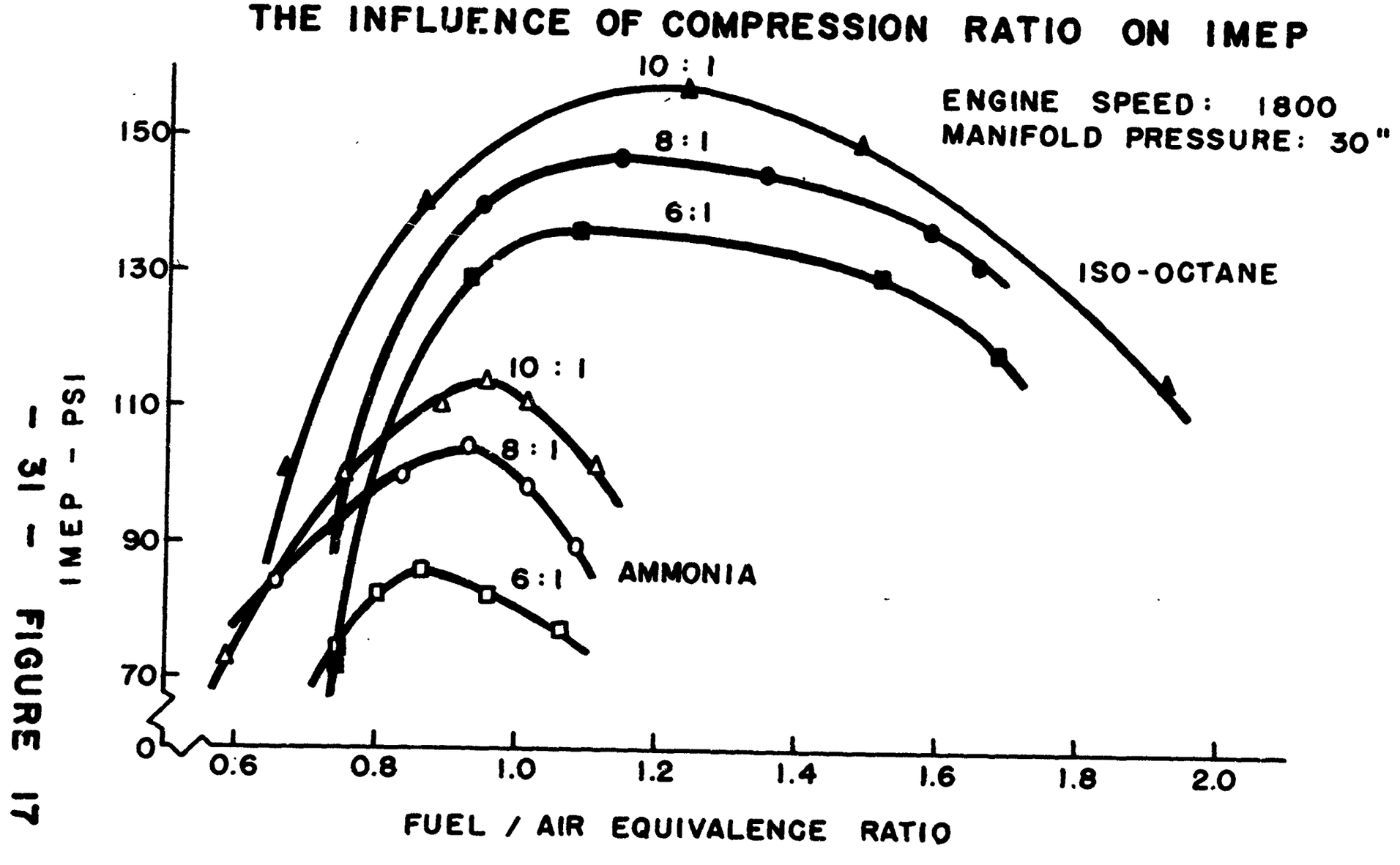
THE INFLUENCE OF COMPRESSION RATIO ON IMEP
ENGINE SPEED: 1800
MANIFOLD PRESSURE: 30"
10 : 1
8 : 1
6 : 1
ISO-OCTANE
10 : 1
8 : 1
6 : 1
AMMONIA
150
130
110
90
70
0
IMEP - PSI
0.6
0.8
1.0
1.2
1.4
1.6
1.8
2.0
FUEL / AIR EQUIVALENCE RATIO

FIGURE 17 - 31 -

THE INFLUENCE OF COMPRESSION ON PEAK PRESSURE

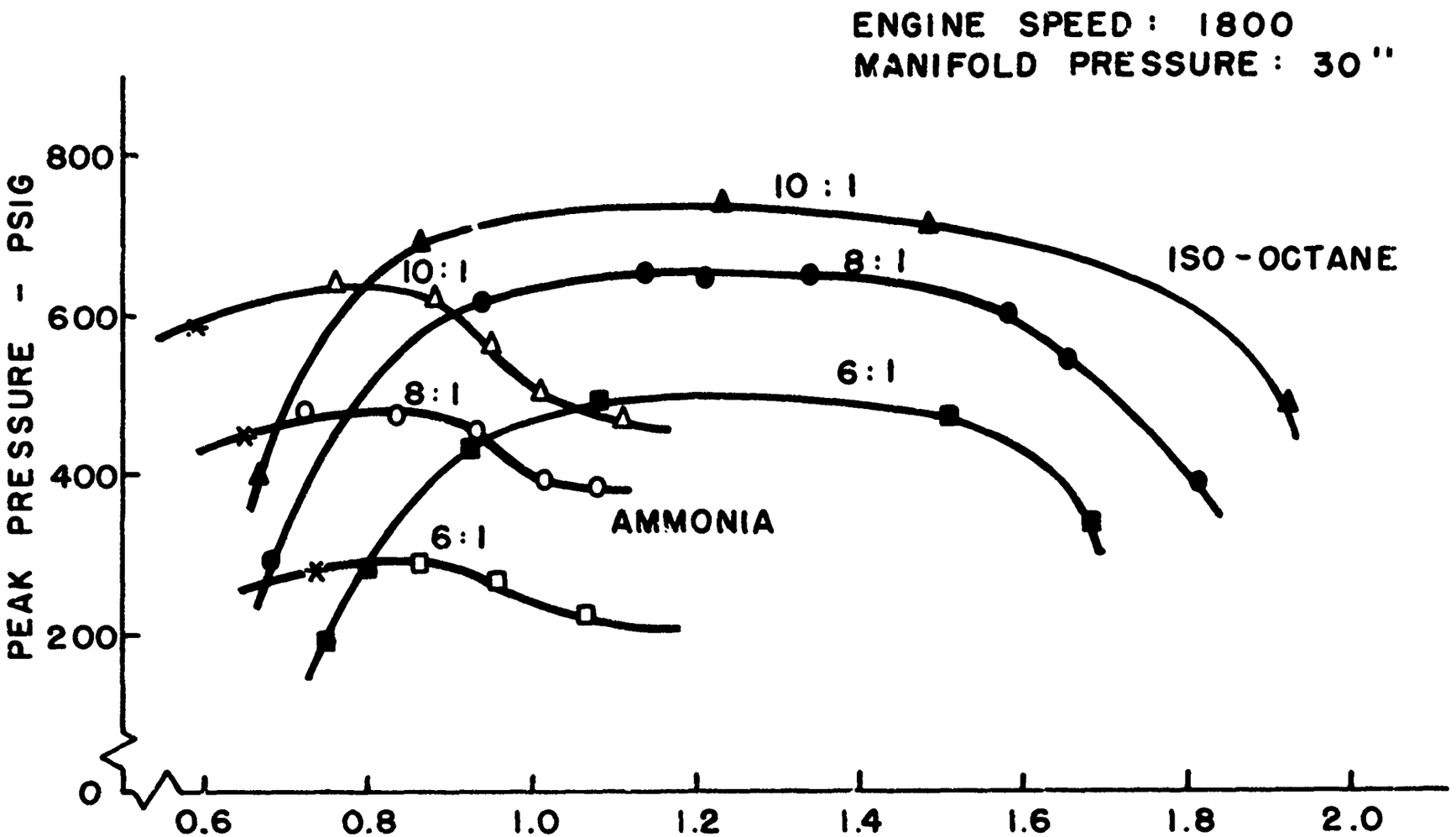

FIGURE 16 - 30 -

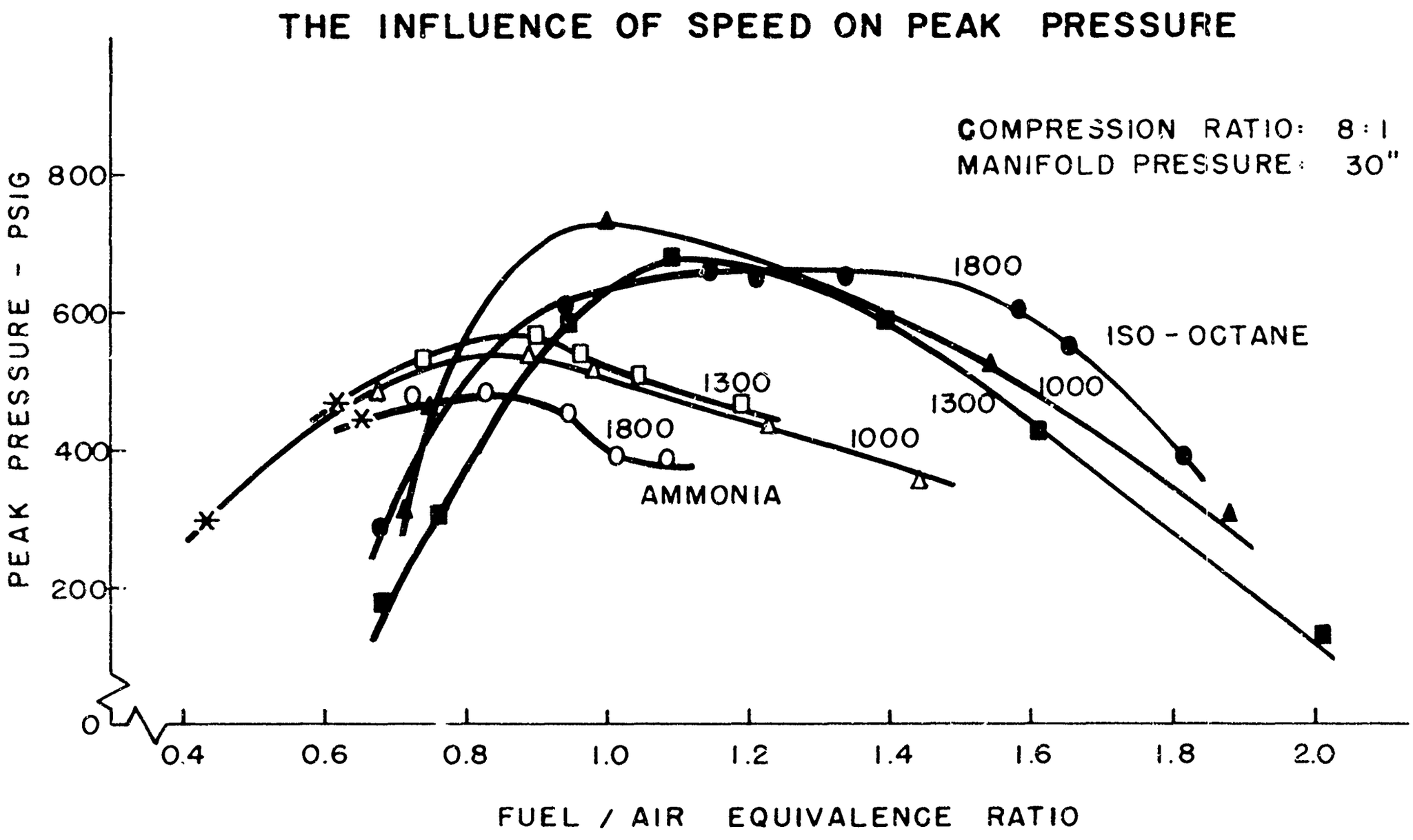
THE INFLUENCE OF SPEED ON PEAK PRESSURE
COMPRESSION RATIO: 8:1
MANIFOLD PRESSURE: 30"
PEAK PRESSURE - PSIG
800
600
400
200
0
1800
ISO-OCTANE
1300
1000
1300
1000
1800
AMMONIA
0.4
0.6
0.8
1.0
1.2
1.4
1.6
1.8
2.0
FUEL / AIR EQUIVALENCE RATIO

FIGURE 19

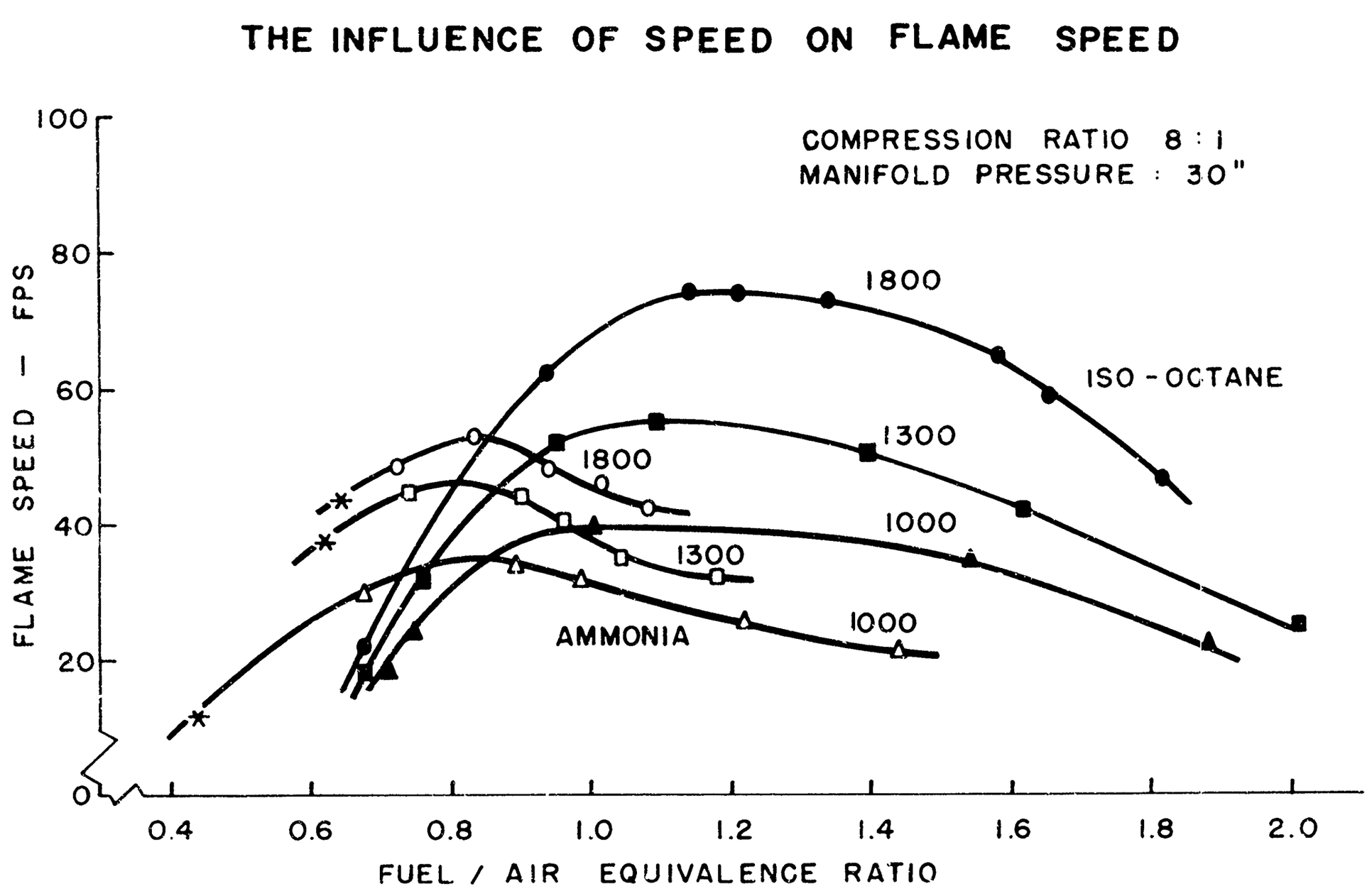
THE INFLUENCE OF SPEED ON FLAME SPEED
COMPRESSION RATIO 8 : 1
MANIFOLD PRESSURE : 30"
FLAME SPEED - FPS
100
80
60
40
20
0
1800
ISO - OCTANE
1300
1800
1000
1300
AMMONIA
1000
0.4
0.6
0.8
1.0
1.2
1.4
1.6
1.8
2.0
FUEL / AIR EQUIVALENCE RATIO

FIGURE 18

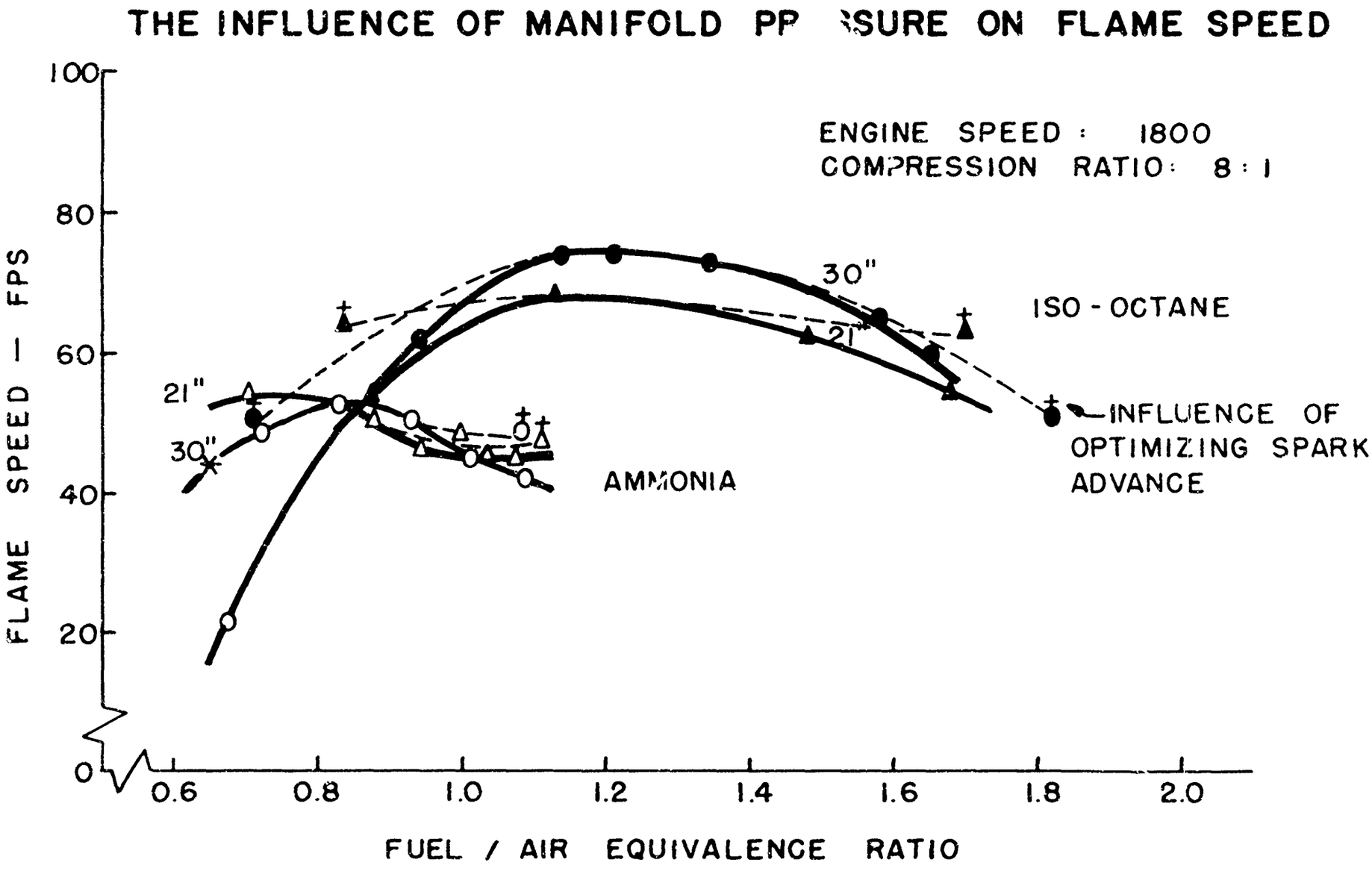
THE INFLUENCE OF MANIFOLD PRESSURE ON FLAME SPEED
ENGINE SPEED : 1800
COMPRESSION RATIO: 8 : 1
FLAME SPEED - FPS
100
80
60
40
20
0
0.6
0.8
1.0
1.2
1.4
1.6
1.8
2.0
FUEL / AIR EQUIVALENCE RATIO
30"
21"
ISO - OCTANE
21"
30"
AMMONIA
INFLUENCE OF OPTIMIZING SPARK ADVANCE

FIGURE 21

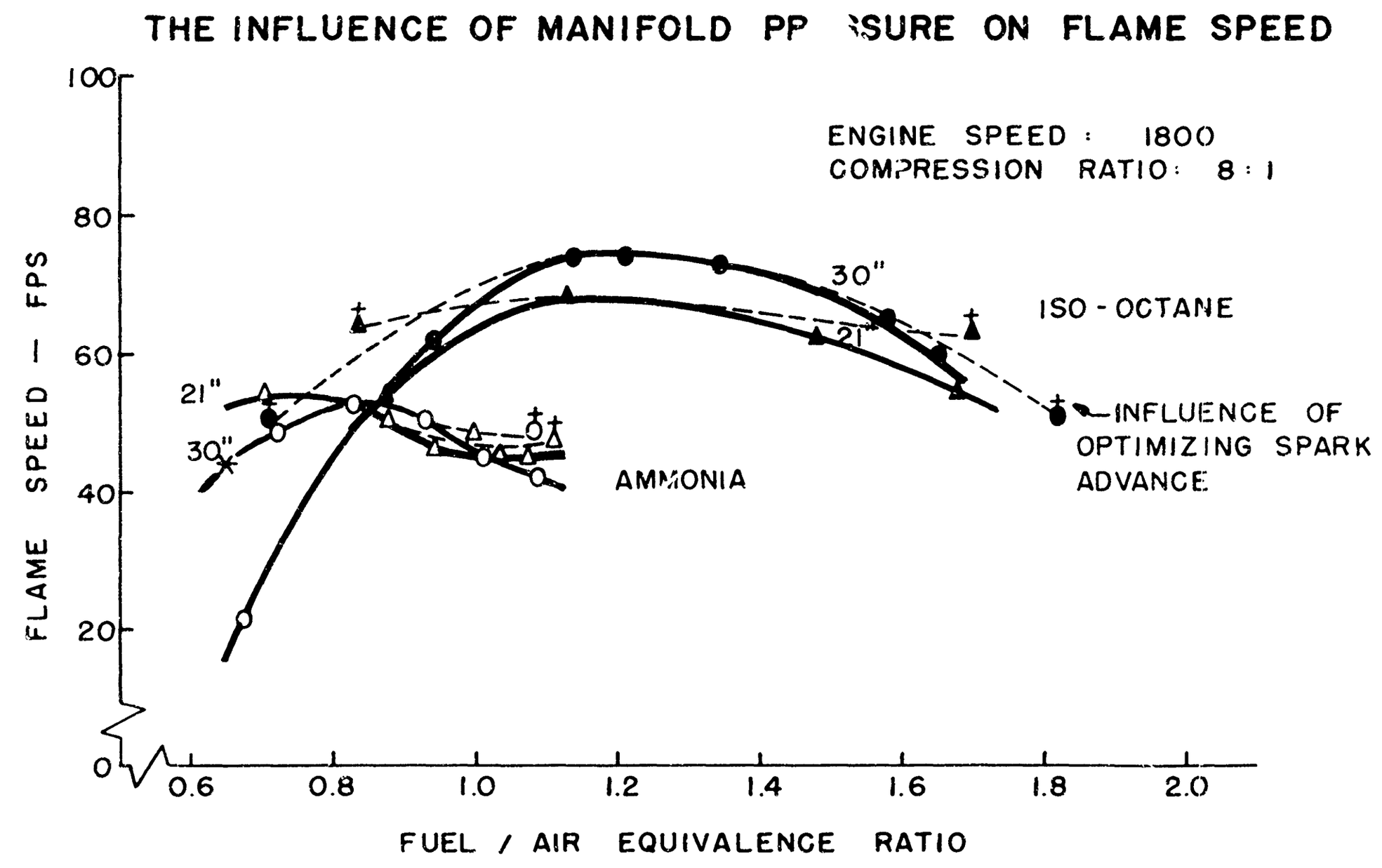
THE INFLUENCE OF MANIFOLD PP SURE ON FLAME SPEED
ENGINE SPEED : 1800
COMPRESSION RATIO: 8 : 1
FLAME SPEED - FPS
100
80
60
40
20
0
30"
21"
ISO - OCTANE
INFLUENCE OF OPTIMIZING SPARK ADVANCE
AMMONIA
0.6
0.8
1.0
1.2
1.4
1.6
1.8
2.0
FUEL / AIR EQUIVALENCE RATIO

FIGURE 21

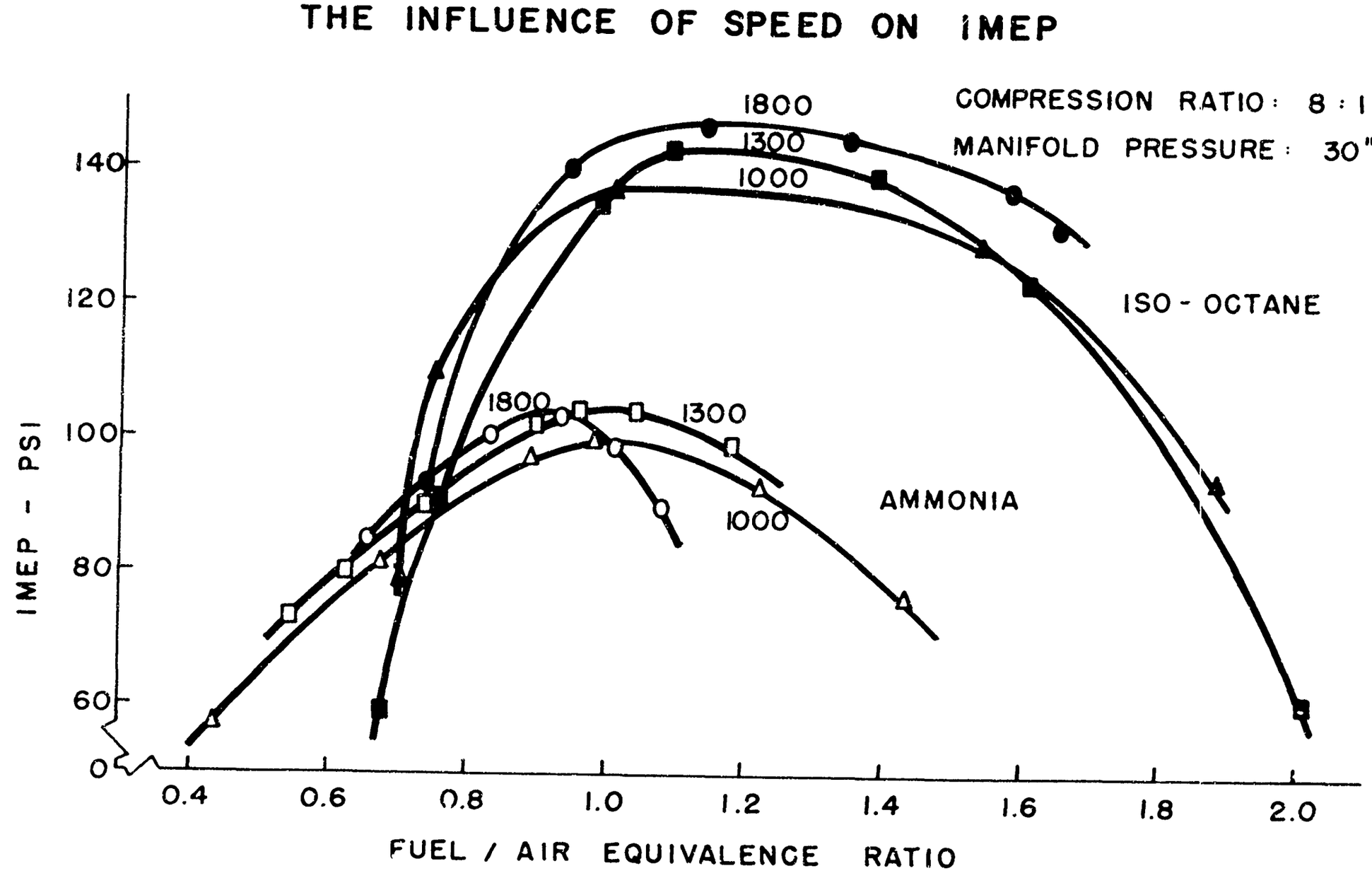
THE INFLUENCE OF SPEED ON IMEP
COMPRESSION RATIO: 8 : 1
MANIFOLD PRESSURE: 30"
1800
1300
1000
ISO - OCTANE
AMMONIA
IMEP - PSI
FUEL / AIR EQUIVALENCE RATIO
0
60
80
100
120
140
0.4
0.6
0.8
1.0
1.2
1.4
1.6
1.8
2.0

FIGURE 20

FUEL / AIR EQUIVALENCE RATIO

THE INFLUENCE OF MANIFOLD PRESSURE ON IMEP

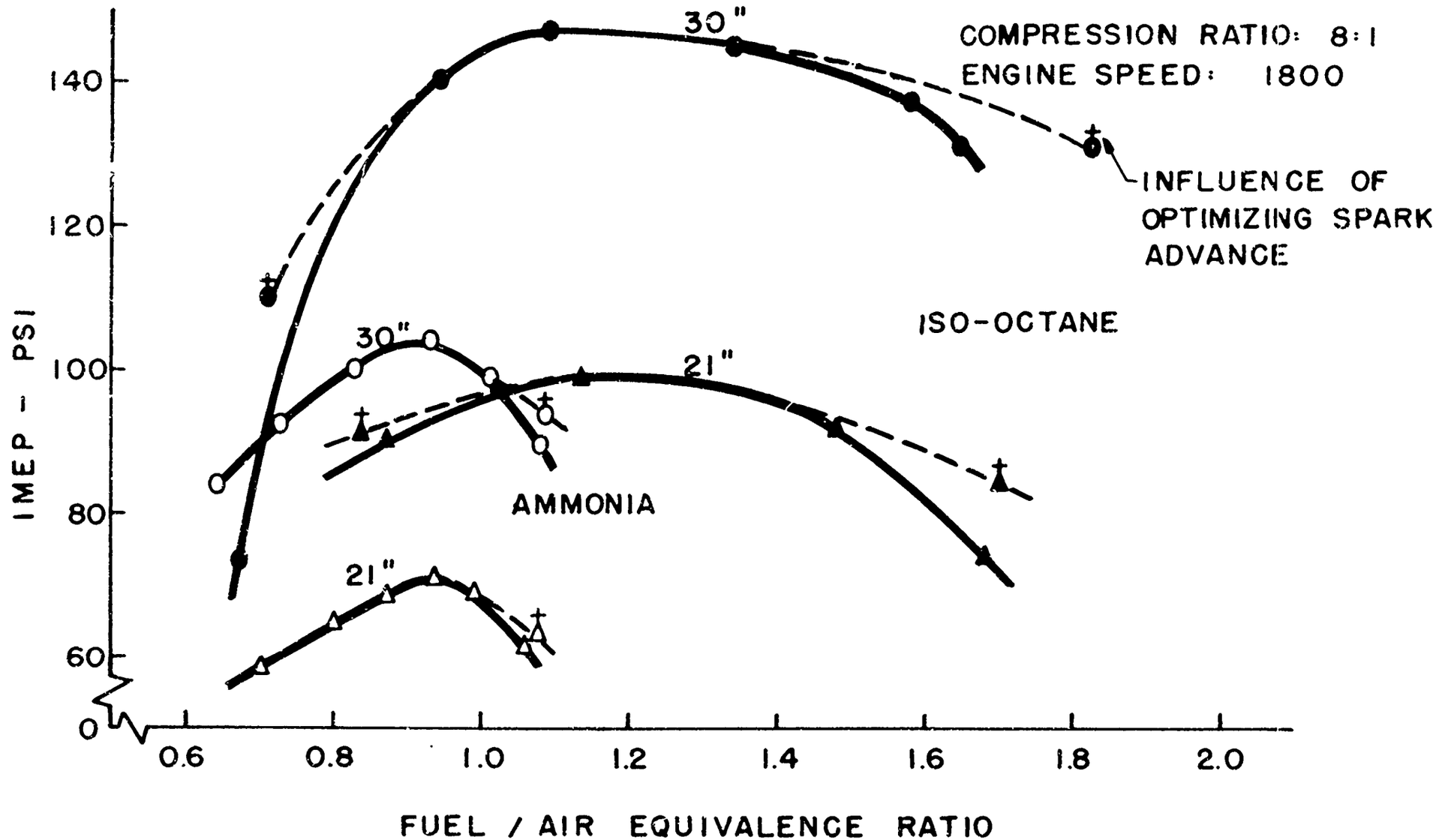

FIGURE 23

THE INFLUENCE OF MANIFOLD PRESSURE ON PEAK PRESSURE AND SPARK TIMING

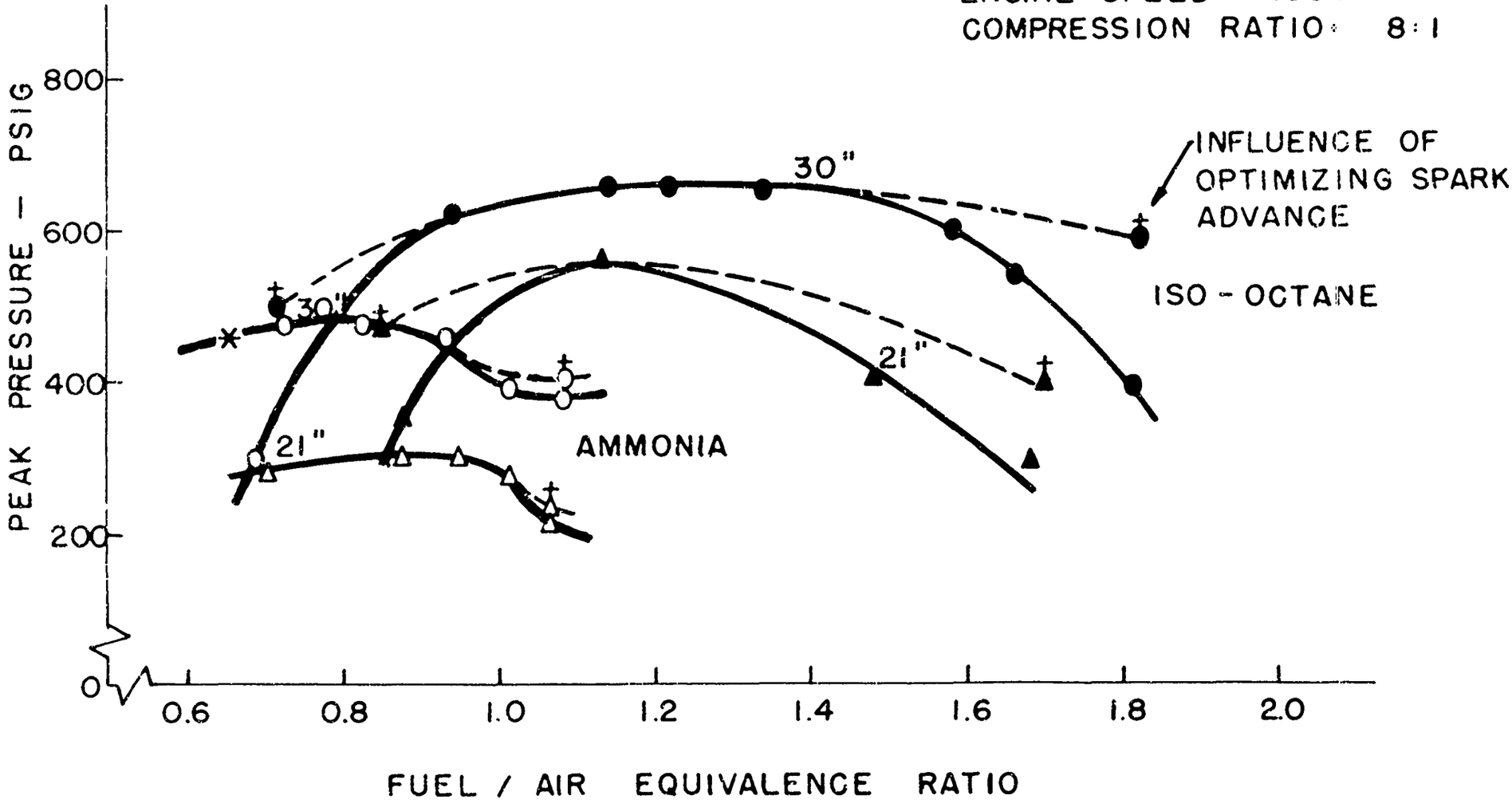

FIGURE 22 - 36 -

THE INFLUENCE OF EQUIVALENCE RATIO ON FLAME SPEED

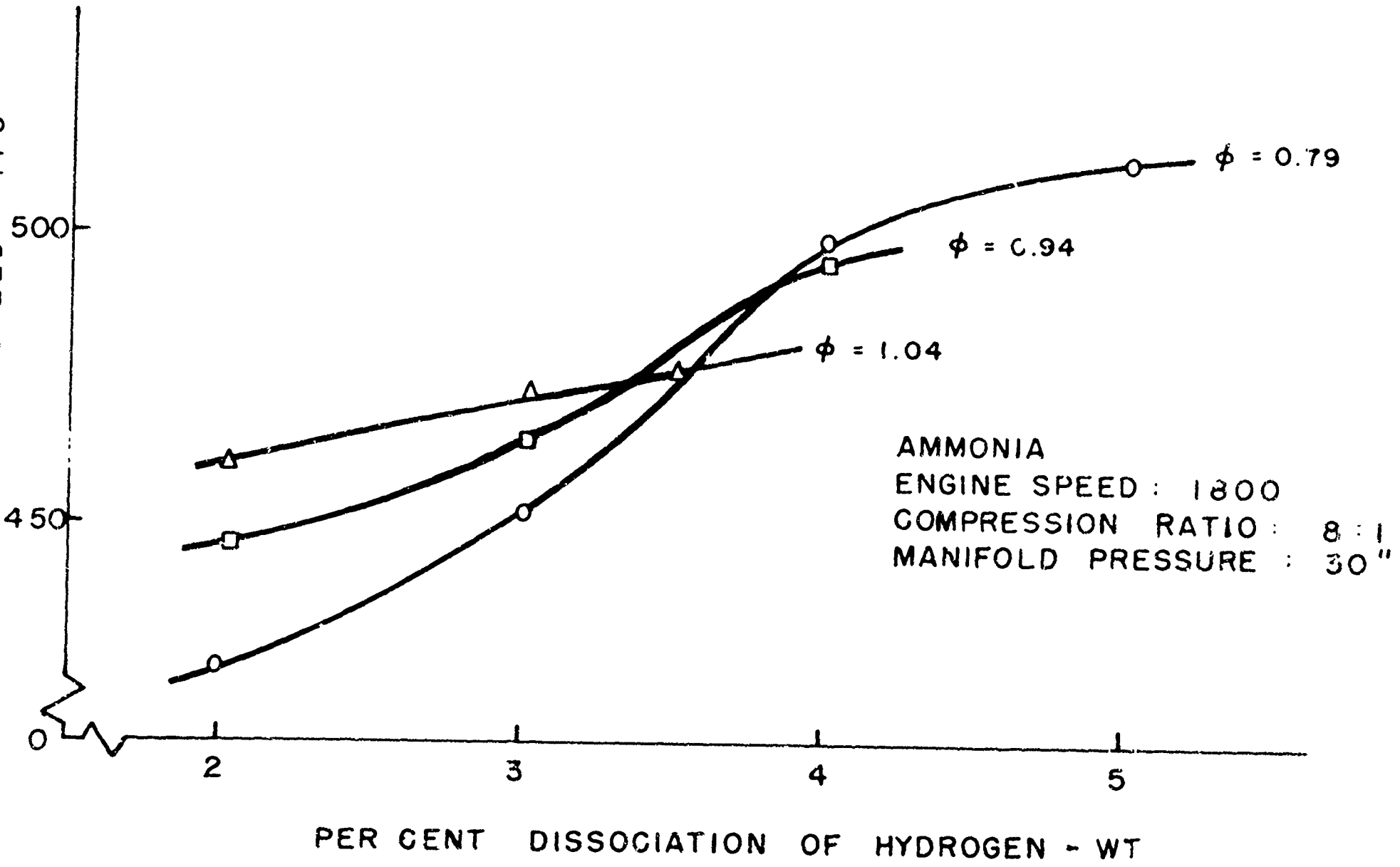

FIGURE 25

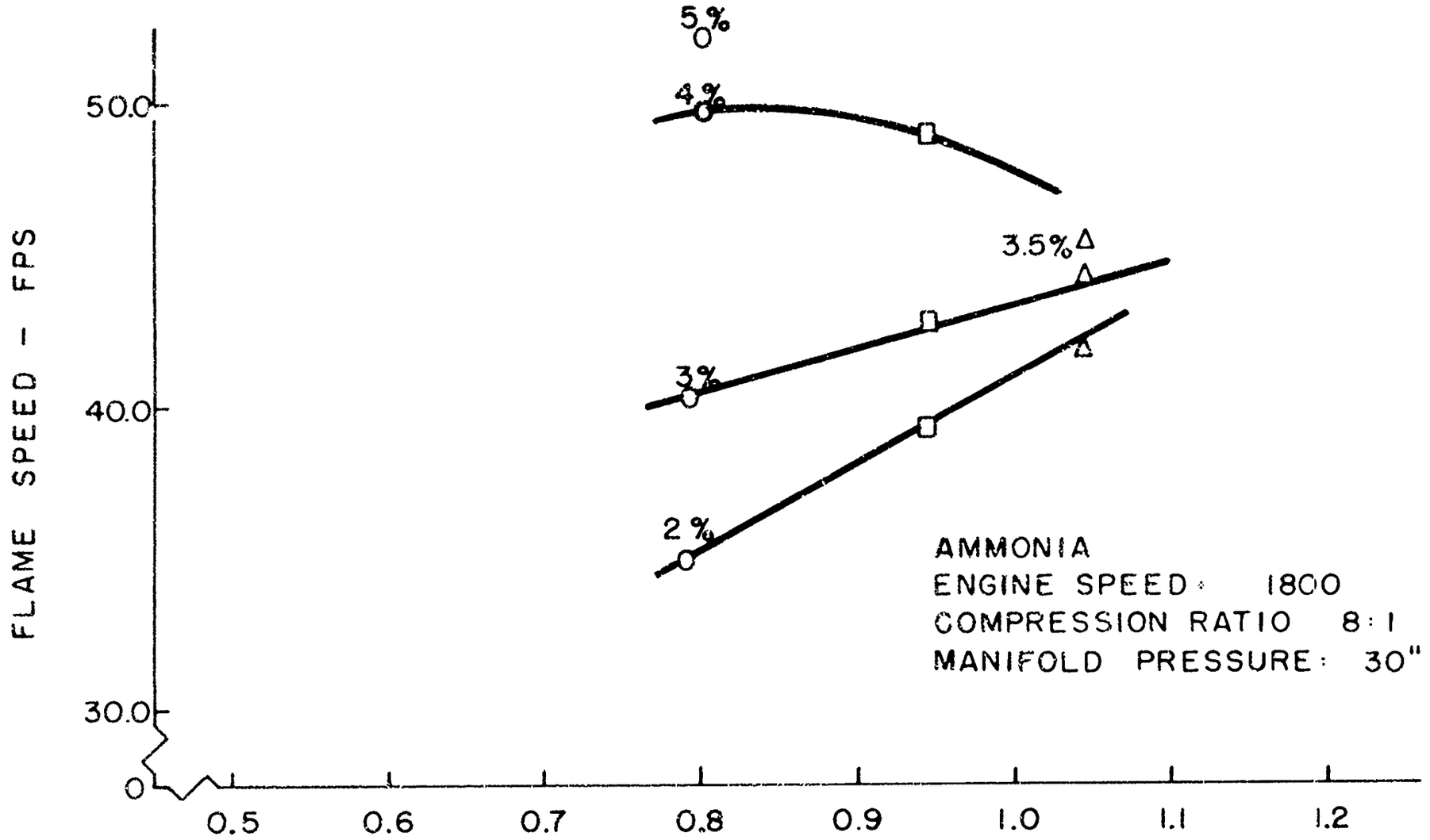
THE INFLUENCE OF DISSOCIATION ON FLAME SPEED
FLAME SPEED - FPS
50.0
40.0
30.0
0
5%
4%
3.5%
3%
2%
AMMONIA
ENGINE SPEED: 1800
COMPRESSION RATIO 8:1
MANIFOLD PRESSURE: 30"
0.5
0.6
0.7
0.8
0.9
1.0
1.1
1.2
FUEL / AIR EQUIVALENCE RATIO

FIGURE 24

TIME - MS

THE INFLUENCE OF EQUIVALENCE RATIO ON PRESSURE AREA (I MEP)

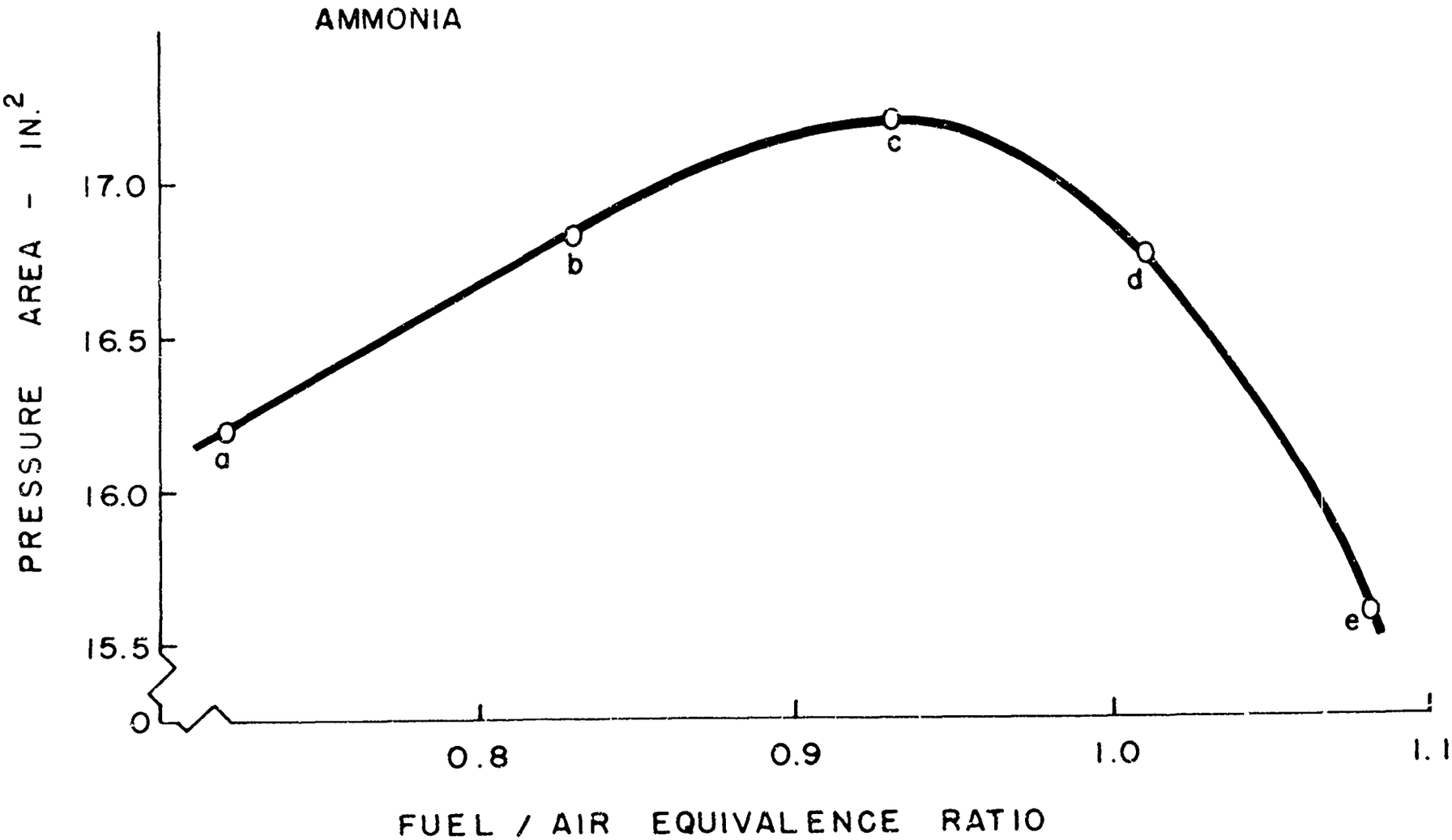

FIGURE 27

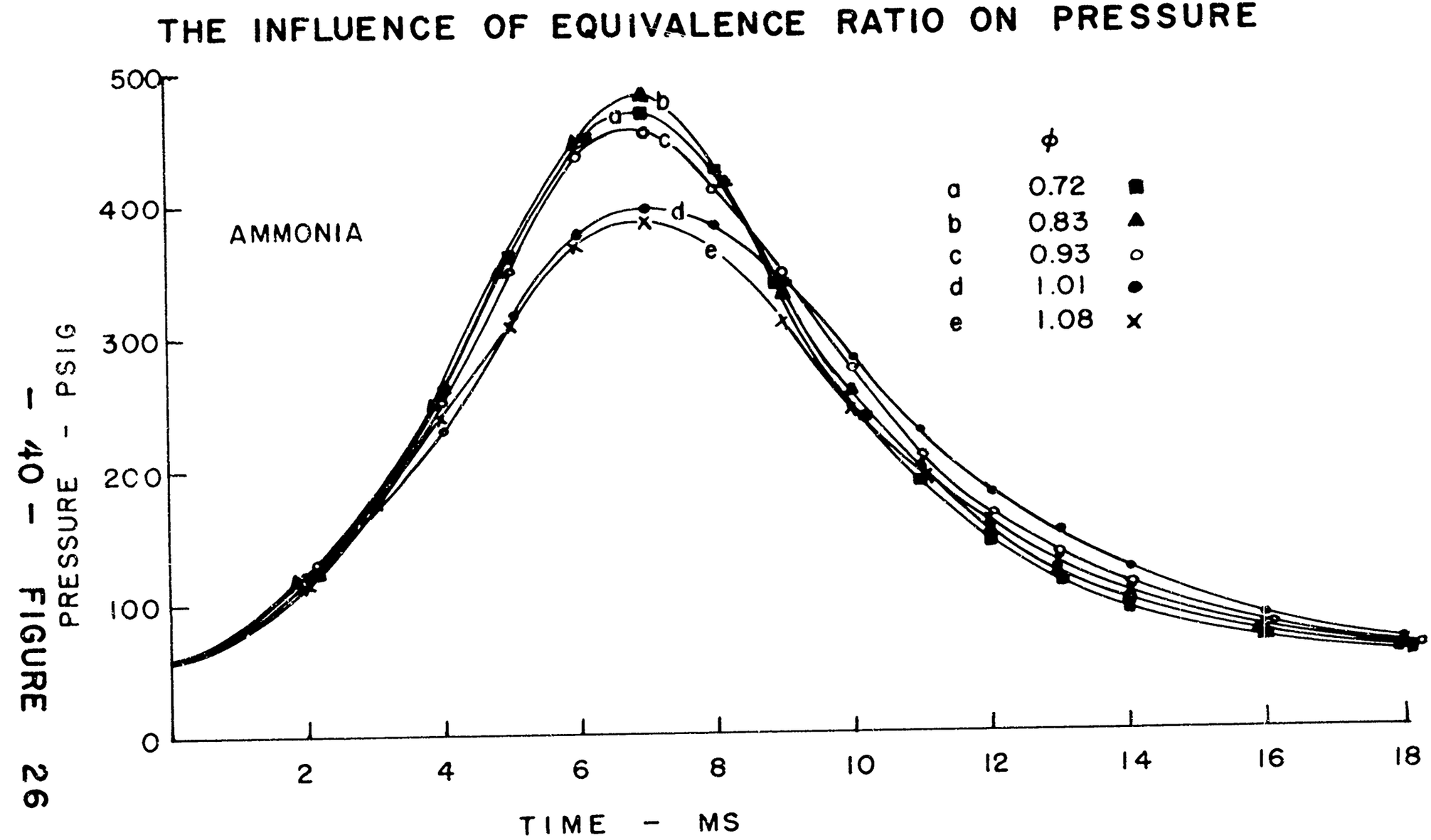
THE INFLUENCE OF EQUIVALENCE RATIO ON PRESSURE
AMMONIA
φ
a 0.72
b 0.83
c 0.93
d 1.01
e 1.08
PRESSURE - PSIG
TIME - MS
0
100
200
300
400
500
2
4
6
8
10
12
14
16
18

FIGURE 26 - 40 -

CONCLUSIONS

1. Ammonia is characterized by a flame propagation rate about 29% slower and an average kernel development time 39% longer than for iso-octane.
2. An increase in compression ratio from 6:1 to 10:1 increases the maximum flame speed of iso-octane 22% from 67.2 fps; and, of ammonia 30% from 44.9 fps.
3. As engine speed decreases from 1800 to 1000 rpm, the flame propagation rates decrease correspondingly: iso-octane, from 74.1 fps to 39.5; and ammonia from 52.5 fps to 33.5.
4. A decrease in manifold pressure from 30 inches of mercury to 21 inches reduced the maximum flame speed of iso-octane 8.5% from 74.1 fps. The maximum for ammonia, however, remained nearly constant at 52 fps which was a reflection upon the apparent controlling factor, ammonia dissociation.
5. The slower flame propagation and longer time for kernel development accounted for the necessity to advance the spark for ammonia nearly twice the 30° value required for iso-octane.
6. It is necessary to maintain the hydrogen dissociation at a value greater than 5% by weight in order to obtain maximum power. This value becomes progressively more critical for lean mixtures.
7. The ammonia flame propagation rates on the lean side are substantially higher (57.4, ϕ = 0.75 compared to 48.5, ϕ = 1.11, fps at 10:1) than on the rich side of maximum power output (occurring at ϕ = .95).

8. The peak pressure varies with the equivalence ratio in a manner identical to the flame speed.

9. It is not possible to increase either the flame speed of the power output for lean mixtures by varying the spark advance, because the controlling factor in combustion behavior was the amount of ammonia dissociated to hydrogen. The optimum amount was realized at all lean conditions.

REFERENCES

1. ASTM Manual of Engine Test Methods for Rating Fuels, American Society for Testing Materials, Baltimore, U.S.A., 1948.

2. Curry, Shelley, "A Three-Dimensional Study of Flame Propagation in a Spark Ignition Engine," E. I. Du Pont de Nemours & Co., Inc., 1962, SAE Paper 452B.

3. Dahm, T. J., "An Investigation of Flame Speeds in a Spark Ignition Engine," M.S. Thesis, University of California, Berkeley, June, 1957.

4. Lewis, B., and Von Elbe, G., Combustion, Flames and Explosions of Gases, Academic Press Inc., New York, 1961.

5. Hodgman, C. D., ed., Handbook of Chemistry and Physics, Chemical Rubber Publishing Co., 45th Edition, 1964-65.

6. Lichty, L. C., Internal Combustion Engines, McGraw-Hill Book Co., New York, 1948.

7. Mukherjee, Fueno, Eyring, and Ree, "Ions in Flames," 8th Symposium (International) on Combustion, Waverly Press, Inc., 1962.

8. Obert, E. F., Internal Combustion Engines, 2nd Edition, International Textbook Co., Scranton, Pa., 1950.

9. Robison, Behrens, and Mosher, "Investigating Rumble in Single-Cylinder Engines," Paper presented at Meeting of the SAE, Atlantic City, June 11, 1958.

10. Shapiro, A. H., The Dynamics and Thermodynamics of Compressible Fluid Flow," Vol. I, Ronald Press Co., 1953.

11. Strange, F. M., "The Relationship Between Equilibrium Temperature and Rate of Pressure Rise in a Spark Ignition Reciprocating Engine," M.S. Thesis, University of California, Berkeley, June, 1958.

12. SAE Journal, "Proposed Nuclear-Powered Energy Depot," p. 27, Vol. 73, No. 4, April, 1965.

13. Van Tiggelen, De Jaegere, and Deckers, "Identity of the Most Abundant Ions in Some Flames," 8th Symposium (International) on Combustion, Waverly Press, Inc., 1962.

APPENDIX A

U-Tube Iso-Octane Fuel Timer:

A U-tube Fuel Timer was adapted to measure the iso-octane flow rates. Water, on the left side of the U-tube (Fig. 28) is balanced by iso-octane in the opposite leg. The water serves as a conducter between various electrodes linking an automated timing circuit. The bottom electrode (D) acts as a common for the other three. When the water contacts the top electrode (A), a solenoid valve shuts off the flow of fuel from the supply tank. The input of fuel is stopped, and the water level decreases due to fuel consumption. As the water detaches from the next electrode (B), the timing clock starts. When the water breaks from the third electrode (C), the clock stops, and the solenoid opens the main filling line. A new cycle is begun and the clock must be reset manually. A reset button on the panel will initiate filling and stop the clock if the need arises.

Calibration of the U-tube Fuel Timer was made by weighing the iso-octane output during one cycle of the clock. This data was repeatable to within $\pm$ 1% and produced fuel/air values to an accuracy of $\pm$ 2.0%.

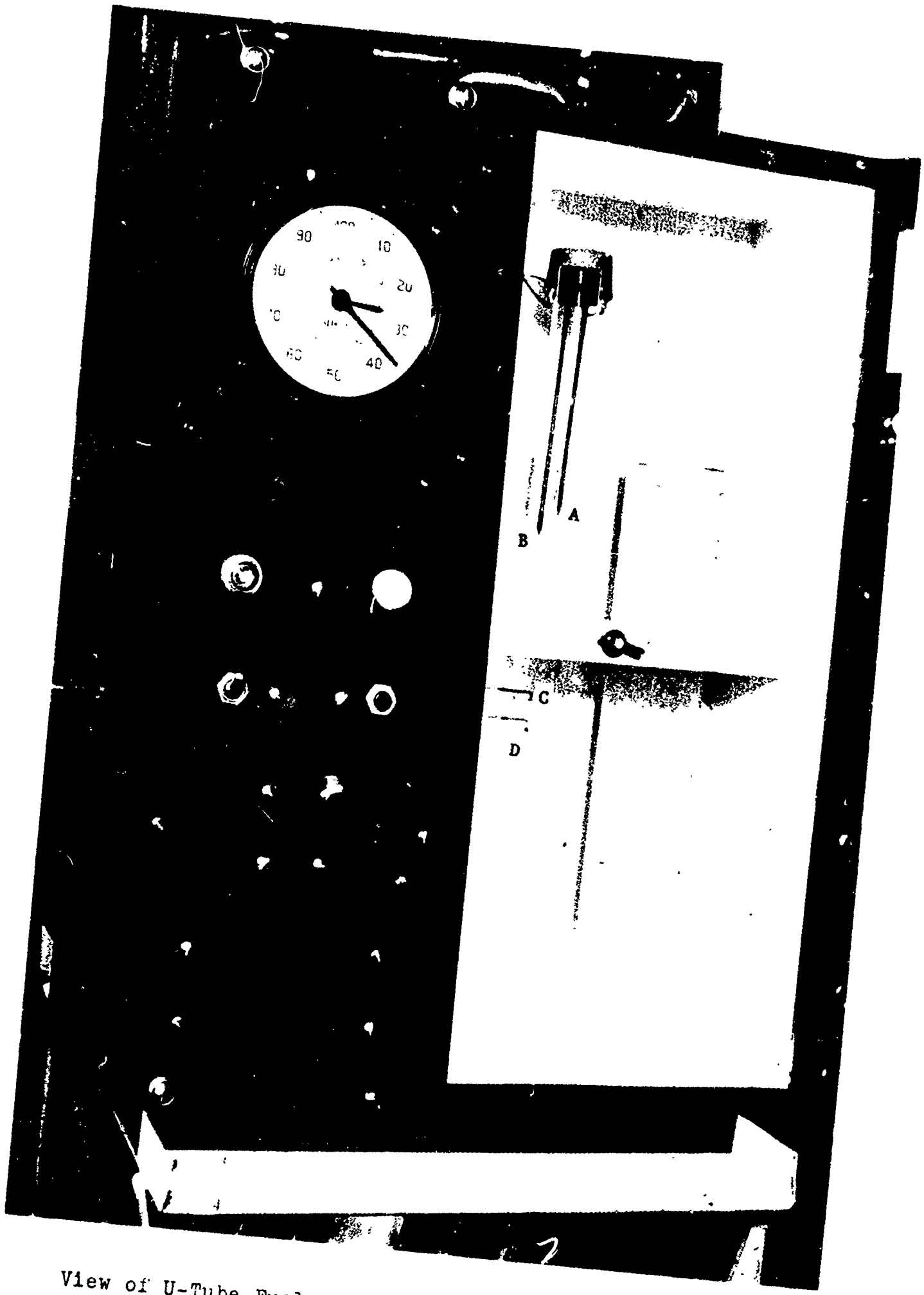

View of U-Tube Fuel Measuring Device

FIGURE 28

APPENDIX B

Ammonia Supply and Metering System:

Figure 29 shows the ammonia supply and metering system. Because ammonia was burned as a vapor, it was necessary to supply heat to the liquid reservoir for vaporization. The steel tank was secured in a bath of water and surrounded with coiled copper tubes supplying both cold water and steam.

The flow of steam is dependent upon the ammonia flow rate and regulated to maintain 120 psig in the tank. The output passes through a regulator (A) that holds a constant pressure downstream (30 psig) for which the metering device was calibrated. The Cox turbine flow meter is shown at point B. The output signal is amplified and read in cycles/second by the counter (C). The thermocouple (D) assures that the vapor does not become superheated due to a low liquid level in the tank. This would render the meter calibration useless because of its temperature dependence.

The valve at location E is used to control the amount of flow which passes into the catalyst chamber (hidden behind the mounting board). Before injecting the ammonia into the manifold of the engine, it is cooled through a heat exchanger to increase the volumetric efficiency of the charge.

The calibration of the ammonia turbine flow meter was made volumetrically from visually recording the variation in the supply tank sight glass. The pressure at the meter of 30 psig was chosen arbitrarily as a value which would produce the necessary flow downstream well within the maximum desired. Repeated calibration checks of the meter showed that the readings were accurate to $\pm$ 1%.

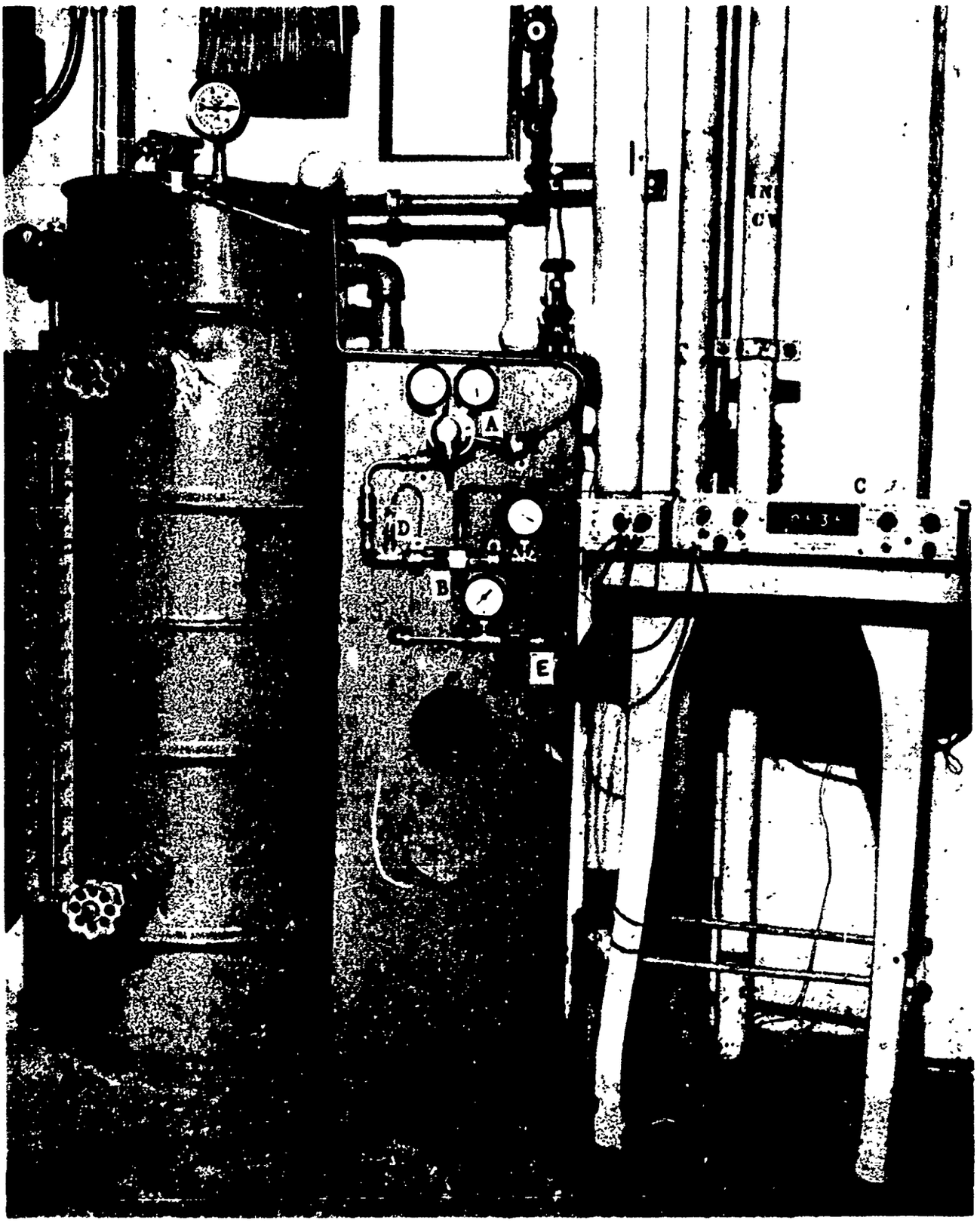

View of Ammonia Supply and Metering System FIGURE 29